OPEN ACCESS

African Journal of Biotechnology

22 May 2019
ISSN 1684-5315
DOI: 10.5897/AJB
www.academicjournals.org

ACADEMIC JOURNALS
expand your knowledge

About AJB

The African Journal of Biotechnology (AJB) is a peer reviewed journal which commenced publication in 2002. AJB publishes articles from all areas of biotechnology including medical and pharmaceutical biotechnology, molecular diagnostics, applied biochemistry, industrial microbiology, molecular biology, bioinformatics, genomics and proteomics, transcriptomics and genome editing, food and agricultural technologies, and metabolic engineering. Manuscripts on economic and ethical issues relating to biotechnology research are also considered.

Indexing

CAB Abstracts, CABI's Global Health Database, Chemical Abstracts (CAS Source Index) Dimensions Database, Google Scholar, Matrix of Information for The Analysis of Journals (MIAR), Microsoft Academic, Research Gate

Open Access Policy

Open Access is a publication model that enables the dissemination of research articles to the global community without restriction through the internet. All articles published under open access can be accessed by anyone with internet connection.

The African Journals of Biotechnology is an Open Access journal. Abstracts and full texts of all articles published in this journal are freely accessible to everyone immediately after publication without any form of restriction.

Article License

Memberships and Standards

Academic Journals strongly supports the Open Access initiative. Abstracts and full texts of all articles published by Academic Journals are freely accessible to everyone immediately after publication.

All articles published by Academic Journals are licensed under the Creative Commons Attribution 4.0 International License (CC BY 4.0). This permits anyone to copy, redistribute, remix, transmit and adapt the work provided the original work and source is appropriately cited.

Crossref is an association of scholarly publishers that developed Digital Object Identification (DOI) system for the unique identification published materials. Academic Journals is a member of Crossref and uses the DOI system. All articles published by Academic Journals are issued DOI.

Similarity Check powered by iThenticate is an initiative started by CrossRef to help its members actively engage in efforts to prevent scholarly and professional plagiarism. Academic Journals is a member of Similarity Check.

CrossRef Cited-by Linking (formerly Forward Linking) is a service that allows you to discover how your publications are being cited and to incorporate that information into your online publication platform. Academic Journals is a member of CrossRef Cited-by.

Academic Journals is a member of the International Digital Publishing Forum (IDPF). The IDPF is the global trade and standards organization dedicated to the development and promotion of electronic publishing and content consumption.

Contact

Editorial Office: ajb@academicjournals.org

Help Desk: helpdesk@academicjournals.org

Website: http://www.academicjournals.org/journal/AJB

Submit manuscript online http://ms.academicjournals.org

Academic Journals
73023 Victoria Island, Lagos, Nigeria
ICEA Building, 17th Floor,
Kenyatta Avenue, Nairobi, Kenya.

Editor-in-Chief

Editorial Board Members

Table of Content

Vol. 18(21), pp. 444-451, 22 May, 2019
DOI: 10.5897/AJB2019.16789
Article Number: 0FE53A860978
ISSN: 1684-5315

http://www.academicjournals.org/AJB

ACADEMIC JOURNALS
expand your knowledge

African Journal of Biotechnology

Full Length Research Paper

Alginate microporous beads promote higher ethanol productivity than the normal beads in a repeated-batch ethanolic process involving *Saccharomyces cerevisiae* LC 269108

Charles O. Nwuche[1,2*], Victor C. Igbokwe[1] and Chukwudi O. Onwosi[1]

[1]Department of Microbiology, Faculty of Biological Sciences, University of Nigeria, Nsukka, 410001, Nsukka, Nigeria.
[2]Biological Resource and Post-Harvest Technology Division, Japan International Research Centre for Agricultural Sciences (JIRCAS), 1-1 Ohwashi, Tsukuba, Ibaraki, 305-8686, Japan.

Received 3 March, 2019; Accepted 30 April, 2019

Mass transfers pose significant challenge in fermentation due to wide diffusion gradient existing between the culture broth and the immobilized cells. In the present study, *Saccharomyces cerevisiae* LC 269108 was immobilized in a recently described microporous alginate beads. The new method was compared with the conventional calcium alginate gel beads in a repeated batch process for the production of ethanol. The fermentation conditions implemented were 110 rpm, pH 5.5 and temperature of 30°C for 60 h. The bead diameters were 3 mm while the calcium chloride concentration was 2.0%. In separate batch experiments conducted by the simultaneous saccharification and fermentation (SSF) method, the free cells maintained plateau at peak ethanol concentration of 7.50±0.33% after 36 h. In the conventional alginate (6.51±0.05%) and microporous beads (7.06±0.10%), ethanol dropped in concentration until reaching final volumes of 5.65±0.33 and 6.56±0.64%, respectively. In the repeated batch experiments, five fermentation batches or runs were conducted over a 12 h period each. The concentrations of ethanol produced in batches with the cells immobilized in calcium alginate were 2.91±0.34, 5.80±0.22, 5.01±0.39, 4.41±0.14 and 3.77±0.21%, respectively. Cells immobilized in microporous beads had higher ethanol output with concentrations 2.33±0.07, 6.62±0.04, 6.16±0.32, 5.90±0.2 and 4.70±0.26% obtained after five respective batches. Glucose metabolism was found to be lower with cells immobilized in alginate beads. From initial glucose concentration of 14.30±0.2%, residual glucose was detected after the first (3.61±2.11%), fourth (3.18±0.98%) and fifth (5.30±0.86%) batches of fermentation. In the batches containing microporous beads, residual glucose (5.36±0.29%) was confirmed after the first batch only. The present study demonstrates the feasibility of using microporous beads in the production of ethanol.

Key words: Mass transfer; microporous beads, immobilized cells, ethanol, calcium alginate.

INTRODUCTION

The apprehension over the ecological issues generated by the wide scale appropriation of anthropogenic energy has propelled researches into the development of alternative energy resources that is cleaner, renewable and environmentally acceptable. Ethanol is an attractive option to fossil fuel because it is a renewable bio-based resource that is oxygenated and reduces emissions from compression ignition engines (Hansen et al., 2005). It is a liquid biofuel, which can be produced from different biomass feedstocks and conversion technologies (Balat et al., 2008). Apart from serving as important source of fuel for automobiles, the demand for ethanol has soared

in recent times due to its extensive applications in medicine, industry and research.

Currently, advancements in fermentation biotechnology have led to the development of immobilized cell systems in bioreactors. Ethanol production using immobilized yeast cells offer several advantages over the free or suspended cell systems. It facilitates cell separation and reuse after fermentation, brings about reduction in adaptation phase and decreases inhibition caused by high concentrations of substrates and products (Lee et al., 2011; Devi and Nagamani, 2018). These attributes promote ethanol production and reduce operating costs (Duarte et al., 2013). Numerous materials such as calcium alginate, agar, polyurethane, polyvinyl alcohol etc., have been investigated as potential immobilization carriers (Rattanapan et al., 2011); but, calcium alginate beads are the most commonly used support because of good biocompatibility, low cost and ease of availability and preparation. Although gel degradation and low mechanical strength are some of the common issues associated with their use, mass transfer limitations remain by far, the most significant challenge encountered with the use of alginate beads as immobilization carriers (Bangrak et al., 2011).

Immobilization in alginate beads leads to the formation of nutrient and oxygen-deficient microenvironments at the core of the gel beads thereby restricting the cells to the periphery of the beads where they are more metabolically active to drive fermentation processes (Oyeagu et al., 2018). The described condition at the core of the beads leads to reduced cell growth rate and productivity of the entrapped cells. Researchers have been developing processes to deal with this problem for some time now. Reduction of the bead sizes (Ogbonna et al., 1991; Perego and Peratello, 1999) and adjusting packed bed bioreactors to higher flow rates (Hussain et al., 2015) are some of their reported approaches. The present study proposes the use of microporous beads as solution to mass transfer limitations in immobilized cells. The term 'microporous' is used to describe the occurrence of microscopic pores or micro-pores on the calcium-alginate gel beads formed by leaching out fillers into the curing solution following the induction of gel formation. The concept and methods of immobilization have been described in a previous paper (Oyeagu et al., 2018). The present study aims to demonstrate the usefulness of microporous beads in the production of bioethanol.

Saccharomyces cerevisiae LC 269108 was immobilized in the conventional alginate beads and compared to those immobilized in microporous beads in terms of ethanol production. The study was conducted in separate cell recycling repeated-batch fermentation mode operated by simultaneous saccharification and fermentation (SSF) using milled dried pulp of decomposing *Dioscorea rotundata* (yam) as feedstock.

The principal raw materials for the commercial production of ethanol are agricultural products, mainly corn and sugarcane (Dias et al., 2015; Eckert et al., 2018). However, many studies reporting the use of starchy tubers like cassava and sweet potato have been published (Lareo et al., 2013; Chutima et al., 2014). Spoilt yam (an agricultural waste) was chosen as feedstock in this study as one way of converting waste to wealth. Due to its high moisture content and short shelf life, yams deteriorate and spoil after a few months of harvest. In Nigeria, for example, nearly 40% of the annual harvested volumes are lost this way. With Nigeria's placement as the world's leading producer and exporter of yams (FAOSTAT, 2017), spoilt yams presently constitute major disposal, public health and environmental problems but the wastes could become useful raw materials in the production of bioethanol. This strategy would help make our environment cleaner, protect the neighborhoods from vector borne pathogens, reduce ethanol production costs, allay the fears of potential food security crises and create jobs. This report presents results of the first study on ethanol production from spoilt yams tubers by repeated-batch SSF with yeast immobilized in microporous alginate beads.

MATERIALS AND METHODS

Yeast strain

The isolation and characterization of the yeast strain, *S. cerevisiae* LC 269108 have been reported (Nwuche et al., 2018). The organism was used as earlier described.

Preparation of the conventional (normal) alginate beads

For the production of the conventional alginate beads, a 2% (w/v) sodium alginate solution was prepared and sterilized by autoclaving at 121°C for 15 min. Then, a 2% (w/v) calcium chloride ($CaCl_2$) was prepared in like manner in a separate beaker. Approximately, 1 ml of overnight culture of the yeast strain grown in YPD10% (1% yeast extract, 2% peptone and 10% glucose) was added to equivalent volume of the cooled sodium alginate preparation and shaken gently to mix. Each milliliter of the cell concentration corresponded to 4.0×10^8 cells/ml. The mixture was then added drop wise into the beaker containing the calcium chloride solution gently stirred at 70 rpm (Magnetic Stirrer OP-912/3, Radelkis, Hungary) using a 5 ml automatic pipette. The alginate droplets solidified upon contact with the solution, forming alginate gel beads. Each bead contained a cell density of approximately 5.0×10^6 cells/bead. Stirring of the resulting beads was continued for 24 h to promote cross linking and stability of the beads (Ogbonna et al., 1989). The beads were recovered and washed in a sterile distilled water to remove excess calcium ion and un-entrapped cells before using in the fermentation

*Corresponding author. E-mail: charles.nwuche@unn.edu.ng. Tel: +2348033728524.

experiments.

Preparation of the microporous beads

For the production of microporous alginate beads, 2% (w/v) sodium alginate was dissolved with 0.4% (w/v) soluble starch in 100 ml of distilled water and sterilized. After cooling, 1 ml of the resulting solution was added to 1ml of the standard cell suspension (corresponding to 4.0×10^8 cells/ml) and twirled gently to homogenize. A sterile 2% (w/v) calcium chloride ($CaCl_2$) solution was prepared in a separate beaker as before. The cells was added to the solution of the soluble starch and sodium alginate and twirled slowly to mix. Using a 1 ml automatic pipette, the resulting mixture was added drop wise into the 2% $CaCl_2$ solution gently stirred at 70 rpm by a magnetic stirrer (OP-912/3 Radelkis, Hungary).The alginate droplets hardened upon contact with the $CaCl_2$ solution, forming gel beads. Each bead corresponded to a cell density of approximately 5.0×10^6 cells/bead. Stirring of the resulting beads was continued (curing) for 24 h to promote cross linking and stability of the beads (Ogbonna et al., 1989). Leaching of the soluble starch occurred at this time leading to development of microscopic pores on the beads (Oyeagu et al., 2018). As described earlier, the gel beads were recovered and washed in sterile distilled water to remove excess calcium and un-entrapped cells before using them in the fermentation experiments.

Sample collection and preparation of rotten yam pulp flour

The yam samples used in this study were handpicked in sterile sample packs from a spoilt farm produce dump and taken to the Crop Science Department, University of Nigeria, Nsukka for taxonomic identification. The tubers were peeled, cut, washed and dried at 80°C for 48 h. The dried yam chips were milled before taking through a horizontally rotating sieve SKH-01 (Fujiwara Scientific Company) having a pore size of 90 µm. The harvested light brown flour was maintained at -30°C until required for use.

Batch SSF of pretreated yam flour and culture conditions

The feedstock (yam flour) was initially subjected to thermal treatment in boiling water for 10 mins to enhance gelatinization/ liquefaction. When cooled to 40°C, enzymatic hydrolysis was initiated with a cocktail composed of amyloglucosidase (46.65 µl), cellulase (0.55 µl) and pectinase (4.21 µl) in order to reduce the viscosity of the paste after the liquefaction regimen. Each batch of SSF experiment comprised of 20% (w/w) pre-treated yam flour mixture in a 50 ml screw capped falcon tube. 0.5 ml of nitrogen base (1% yeast extract and 2% peptone) was added before the medium was aseptically inoculated with the immobilized (calcium alginate or microporous beads) or standardized 1 ml overnight culture of the yeast strain. The concentration of the inoculum was 4.0×10^8 cells/ml. The set-up was incubated at 30°C for 12 h. Approximately, 100 µl samples were withdrawn two hourly from the sealed fermentation tubes, transferred into 1.5 ml Eppendorf tubes and preserved at -30°C until analyzed for ethanol and glucose.

Repeated-batch SSF of pre-treated yam flour

In the repeated-batch SSF, after the 12 h batch fermentation described in the previous section, the immobilized cells were retrieved by filtration through a sterile mesh sieve (2 mm). The collected cells were then reused for the next batch of fermentation, and the process was repeated five times according to the method described by Watanabe et al. (2012).

Analytical methods

The proximate composition of the yam flour used was determined according to Standard Methods (2005). The maximum theoretical ethanol yield from sugar was calculated from the stoichiometric relation according to Siqueira et al. (2008): 100 g of hexose produces 51.1 g of ethanol and 48.9 g of CO_2. The theoretical ethanol yield was calculated from the following equation:

Theoretical ethanol yield (%) = Ethanol Conc. (%) / Glucose Conc. (%) × 100

Glucose was monitored using High Performance Liquid Chromatography system (TOSOH, Tokyo, Japan) while ethanol was determined by a gas chromatography (Model GC-2014; Shimadzu Seisakusho, Kyoto, Japan). The operating conditions of the equipment were reported in Nwuche et al. (2018).

Statistical analysis

All reported experiments were conducted in triplicates. The standard error of mean was calculated and the mean values plotted at 95% confidence limit against the days of fermentation. Ethanol production in batch experiments was compared using one way analysis of variance (ANOVA).

RESULTS AND DISCUSSION

Batch SSF of 20% (w/v) flour from dried yam pulp

SSF is a commonly employed microbial technique for the production of bioethanol. It is a one-step fermentation method that involves conversion of glucose to ethanol in the same vessel with reduction in fermentation time, decrease in capital cost and increase in production of ethanol (Sarkar et al., 2012; Dey et al., 2015) as some of its attractive advantages. Many fermentation systems operate a repeated fed-batch operation with SSF in a cell-recycling mode. To this extent, the use of flocculating and immobilized cells have been reported in the fermentations of cassava starch (Amuthaa and Gunasekaran, 2001; Choi et al., 2009) and lignocellulosic materials such as rice straw (Watanabe et al., 2012). Ethanol production by the free and immobilized (alginate and microporous) cells was conducted by separate batch SSF ahead of the repeated batch experiments. In Figure 1, the kinetics of ethanol concentration by the three (free cells, microporous immobilized and normal alginate immobilized cells) different cells is presented. Ethanol concentration in the batch inoculated with free cells reached 7.12±0.13% (87.2% of the theoretical yield) after 12 h and gradually increased further to 7.50±0.33% (90.73% of the theoretical yield) after 36 h before maintaining plateau for the rest duration of the experiment. In contrast, ethanol produced from the cells immobilized in alginate and microporous beads reached

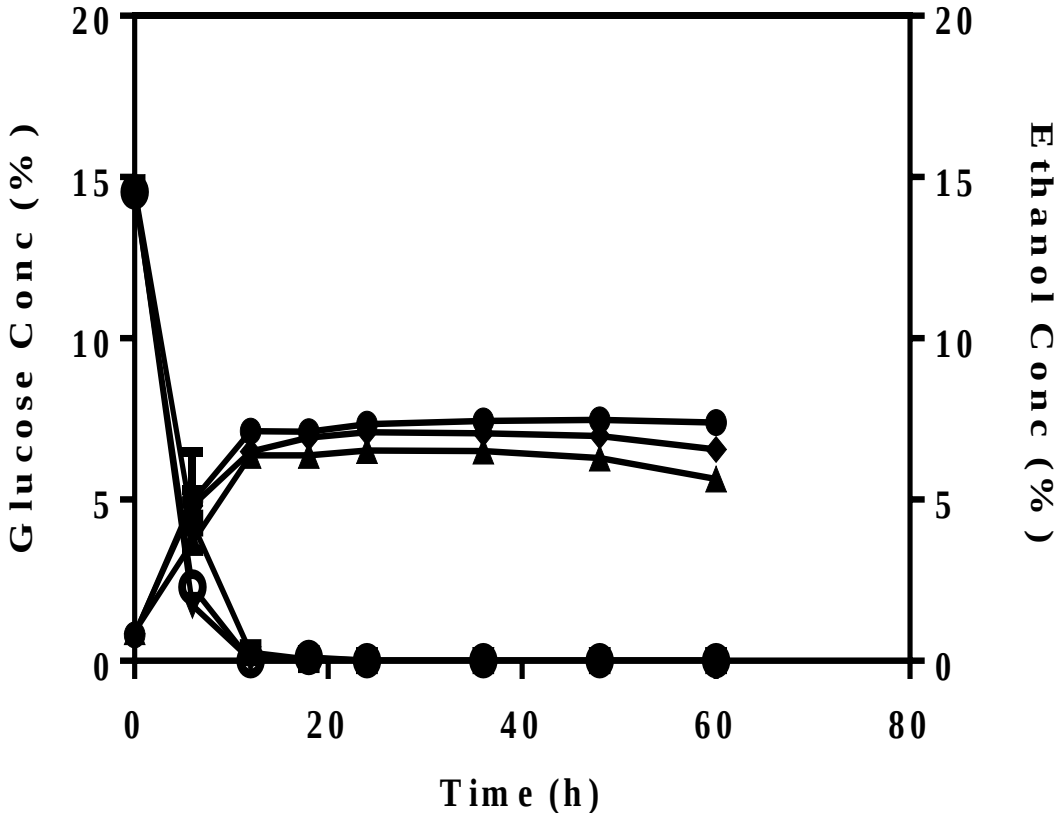

Figure 1. Batch profiles of ethanol production and glucose consumption with 20% (w/v) yam flour using *Saccharomyces cerevisiae* LC269108. Ethanol conc % (free cells), glucose conc % (free cells), ethanol conc % (cells in normal alginate beads), glucose conc % (cells in normal alginate), ethanol conc % (cells in microporous beads), glucose conc % (cells in microporous beads).

peak after 36 h and thereafter dropped in concentration. In the culture inoculated with cells immobilized in normal alginate, for instance, the ethanol concentration was 6.37±0.08% (76.7% of theoretical yield) after 12 h. This concentration increased to 6.51±0.05% (78.4% of theoretical yield) after 36 h before dropping to 5.65±0.33% (68% of theoretical yield) at the end of experiment. The batch containing cells immobilized in microporous beads had higher ethanol output than the batches, which had the conventional alginate beads. After 12 h, the concentration of ethanol produced was 6.49±0.49% (78.7% of theoretical yield) before it increased to 7.06±0.10% (85.6% of theoretical yield) after 36 h. The final ethanol concentration after 60 h was 6.56±0.64% (79.6% of the theoretical yield).

Many studies have indicated the numerous advantages of immobilized cultures in the production of ethanol. Besides the benefits of easier separation from the reaction mixture, possibility of cell reuse and higher substrate conversion, ethanol production have also been reported to be higher than when free cells were used (Puligundla et al., 2011; Yao et al., 2011). However, results obtained in the present study indicated otherwise. The concentration of ethanol produced by the free cells was higher compared to those produced by the immobilized cells. This position is shared by Duarte et al. (2013). Such difference is explainable by mass transfer limitations occurring within the immobilization matrix. Alginate beads are known to maintain two distinct spheres or regions, the core of the beads, which is characteristically anaerobic and farthest way from the culture broth and the periphery where the cells are most metabolically active due to increased access to medium materials (Oyeagu et al., 2018). During fermentation, the cells located at the core are relatively inactive and thus contributes insignificantly to fermentation due to limitations imposed by the absence of the medium resources. The microporous beads were found to be beneficial to higher ethanol production than the normal alginate beads because the micropores formed as result of the leaching of starch during preparation facilitated movement of nutrients even to the core of the beads.

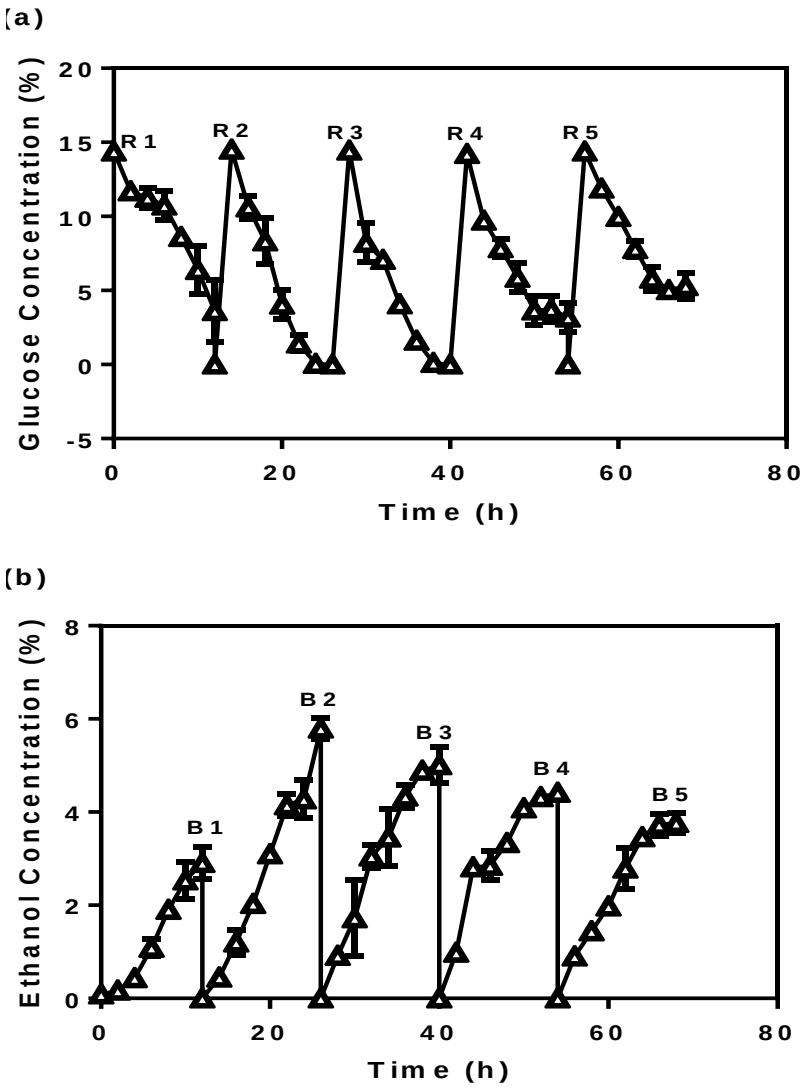

Figure 2. Repeated batch fermentation profiles using 20% (w/v) yam flour as feedstock – (a) ethanol production and (b) glucose consumption by *S. cerevisiae* LC 269108 immobilized in conventional alginate beads.

This ensures net flow of materials because nutrients and oxygen are delivered to all parts of the beads while metabolic wastes are channeled back to the culture medium. The microporous beads thus tend to hold much higher concentration of metabolically active cells than those immobilized in conventional alginate beads. This explains the higher concentration of ethanol produced by the former.

Repeated batch SSF of the 20% (w/v) flour from dried yam pulp

To evaluate the adaptation of the microporous beads to prolonged fermentation, a cell recycling repeated batch SSF was carried out and compared to the alginate beads. Five repeated batches were run at 12 h intervals. The time interval was chosen because glucose was found to completely exit the system within 12 h of fermentation. Samples were withdrawn for analysis in 2 h. The kinetics of ethanol and glucose fermentation is presented in Figures 2 and 3. In the batch SSF experiment with cells immobilized in alginate beads, ethanol production reached peak of 2.91±0.34% (38.9% of the theoretical yield) in the first batch of experiment. In the second batch (B 2), ethanol increased to 5.80±0.22% (73.9% of the theoretical yield) before dropping to 5.01±0.39% (60.3% of the theoretical yield) and 4.41±0.14% (52.6% of the theoretical yield) in the third and fourth batches respectively. The concentration decreased further to

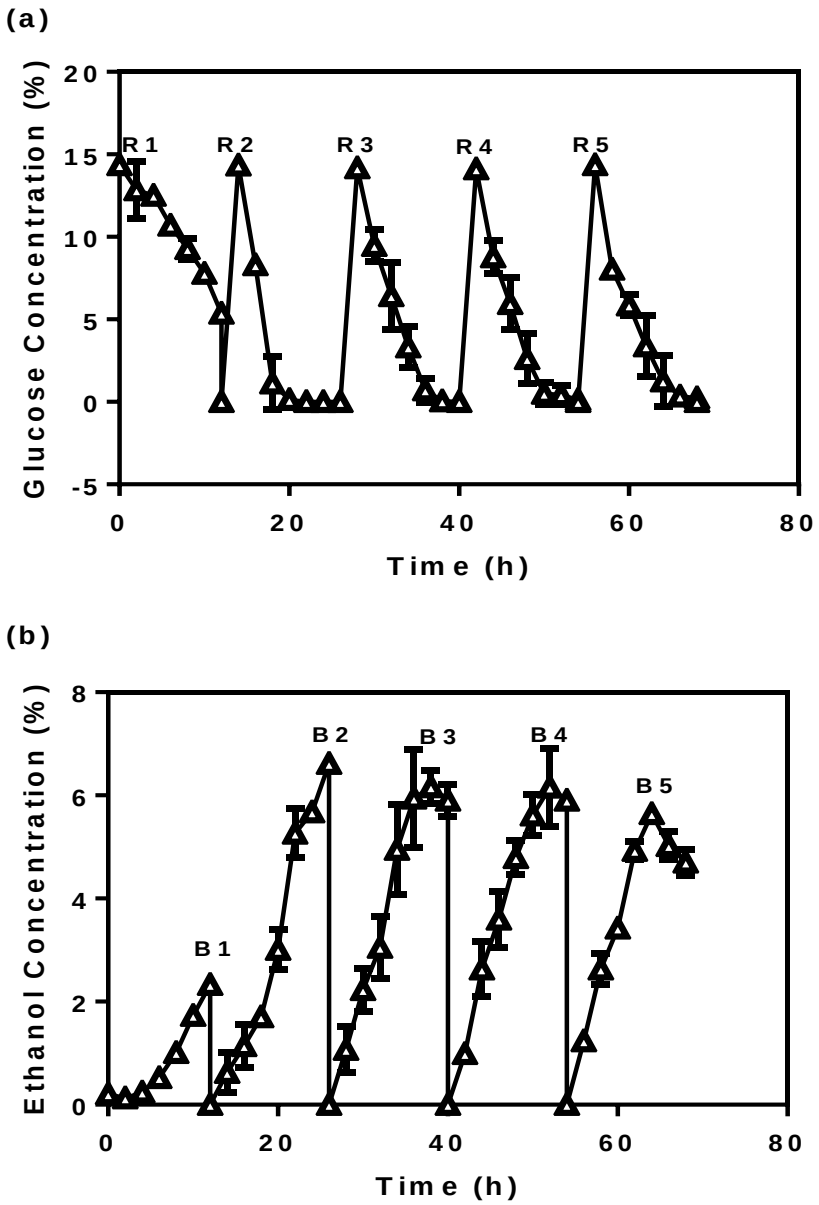

Figure 3. Repeated batch fermentation profiles using 20% (w/v) yam flour as feedstock – (a) ethanol production and (b) glucose consumption by *S. cerevisiae* LC 269108 immobilized in microporous alginate beads.

3.77±0.21% (45.4% of the theoretical yield) in the final batch of experiment. Time courses of experiment equally revealed that ethanol concentration at zero hour followed an increasing order from the first batch of experiment to the last. In the first batch, the concentration of 0.092% was observed. Subsequently, higher values were obtained in the second (0.4526%) and other batches. Values obtained before the third (0.914%) and fourth (0.983%) batches commenced were comparable. The fifth batch profile showed 1.128% ethanol concentration prior to fermentation.

In the batches of experiment with cells immobilized in microporous beads (Figure 3b), maximum ethanol production after the first batch was 2.33±0.07% (30.6% of the theoretical yield). This value increased significantly to 6.62±0.04% (82.5% of the theoretical yield) in Batch 2 (B 2) before dropping to 6.16±0.32% (B 3) and 5.90±0.02% (B 4) respectively. The calculated theoretical yields were 72.7 and 69.7% respectively. Ethanol production in the fifth batch was lowest (4.70±0.26%) with 55.27% theoretical yield. As earlier indicated, ethanol concentration at zero hour increased progressively in concentration across the different batches of experiment. For instance, from an initial 0.213% in the first batch, the

concentration increased to 0.620% (B 2), before the values for the third (1.07%) and fourth (0.99%) batches were determined. The concentration of ethanol before fermentation of the final batch was 1.23%. Such increments in the zero hour concentration of ethanol across the batches might have come from two possible sources. The first is the broth remnants adhering to the immobilizing beads from the previous fermentation run and second is the absence or reduction in adaptation phases during the successive batches of experiment (Duarte et al., 2013). From the present study, ethanol decreased subsequently after reaching peak in the second batch. This observation was common to both alginate and microporous beads (Figure 2b and 3b) and may have arisen from loss of cells due to breakage or leakages from the beads (Bangrak et al., 2011). One of the limitations of the alginate beads is their low mechanical strength (Watanabe et al., 2012). It is thought that abrasions resulting from agitations during fermentation weakens and ruptures the beads. In terms of ethanol output, the cells immobilized in microporous beads were significantly better ($p<0.05$) than the performance of those immobilized in alginate beads particularly from the second to the fifth batches of fermentation. Apart from improvement in mass movement of medium materials, the microporous beads were physically more stable than the normal beads. The first reason is due to increased penetration of $CaCl_2$ to the core of the beads. This results in the formation of more cross-linkages between carboxyl groups in the alginate with the calcium ions from the chloride solution. Consequently, calcium progressively accumulates in the beads bringing about a hardening effect. Secondly, earlier report (Oyeagu et al., 2018) showed that incorporating 0.4% starch during preparation of the microporous beads adds significantly to increased stability and cell holding capacity of the resulting beads than any other concentration or fillers tested. Watanabe et al., (2012) and Duarte et al. (2013) have equally reported a variety of techniques aimed at strengthening and fortifying alginate beads with the aim of achieving longer term applications during fermentation.

Glucose metabolism was observed to be lower with cells immobilized in normal alginate beads (Figure 2a). At the end of the first batch of experiments, the residual concentration of glucose was found to be 3.61±2.11%. This remnant might account for the adaptive or lag phase response, which normally occurs when microbial cells are acclimatizing to the physical conditions of a fermentation system. In the second and third batches, glucose was not detected in the broth. Residual glucose emerged again in the fourth (3.18±0.98%) and fifth (5.30±0.86%) batches respectively. Cell loss could also in part account for the residue glucose but it is known that the activity of cells immobilized in conventional alginate is restricted to the peripheral zones where limited concentration of cells is located. In the microporous beads, glucose consumption was faster (Figure 3a). After the unconsumed concentration of 6.36±1.12% was found at the completion of the first batch, glucose was not detected again in the other batch profiles of experiment. This confirms further that a higher and more robust consortium of metabolically active cells resided in the microporous beads than in the normal alginate.

Conclusion

In the present study, microporous beads was investigated as potential solution to mass transfer challenges using ethanol production as case study. The results showed improvement in mass movement as indicated by the higher product concentrations achieved using the microporous beads. However, additional studies are needed to optimize the process in order to determine the set of conditions most beneficial to the ethanol fermentation. Many factors such as incubation temperature, initial pH and sugar concentration are known to influence growth and ethanol production in yeasts. Although the addition of 0.4% starch improved stability of the resulting beads, further research is obligatory in order to develop newer options for improving the stability and strength of the beads to enable them become more adaptable to longer fermentations periods. Also, contamination of culture did not occur despite using the feedstock (prepared from putrefying yam tuber) without sterilization. The reasons for this might be due to rapid consumption of glucose by the yeast, the high concentration of ethanol produced and the adaptation of the yeast strain (*S. cerevisiae* LC 269108) to the high temperature of fermentation. The significance of this to savings in energy and overall cost of production is very critical for large scale production of ethanol.

CONFLICT OF INTERESTS

The authors have not declared any conflict of interests

ACKNOWLEDGMENTS

This work was supported by funding from the ministry of Agriculture, Forestry and Fisheries of Japan (Development of climate change mitigation technology through effective utilization of agro-processing residues). The authors wish to appreciate the Japan International Research Centre for Agricultural Science (JIRCAS) for funding the work.

REFERENCES

Amuthaa R, Gunasekaran P (2001). Production of ethanol from liquefied cassava starch using co-immobilized cells of *Zymomonasmobilis* and *Saccharomyces diastaticus*. Journal of Bioscience and Bioengineering 92(6):560-564.

Balat M, Balat H, Oz C (2008). Progress in Bioethanol Processing. Progress in Energy and Combustion Science 34(5): 551-573.
Bangrak P, Limtong S, Phisalaphong M (2011). Continuous ethanol production using immobilized yeast cells entrapped in loofa-reinforced alginate carriers. Brazilian Journal of Microbiology 42(2):676-684.
Choi GW, Kang HW, Moon SK (2009). Repeated-batch fermentation using flocculent hybrid, *Saccharomyces cerevisiae* CHFY0321 for efficient production of bioethanol. Applied Microbiology and Biotechnology 84(2):261-269.
Chutima K, Dethoup T, Limtong S (2014). Ethanol production from cassava using a newly isolated thermotolerant yeast strain. Science Asia 40:268-277.
Devi NKD, Nagamani ASS (2018). Immobilization and estimation of activity of yeast cells by entrapment technique using different matrices. International Journal of Pharmaceutical Sciences and Research 9(7):3094-3099.
Dey P, Lhakpa W, Singh J (2015). Simultaneous saccharification and fermentation (SSF), an efficient process for bio-ethanol production: an overview. Biosciences Biotechnology Research Asia 12(1):87–100.
Dias MOS, Filho RM, Mantelatto PE, Cavalett O, Rossell CEV, Bonomi A, Leal MRLV (2015). Sugar cane processing for ethanol and sugar in Brazil. Environmental Development 15:35-51.
Duarte JC, Rodrigues JAR, Moran PJS, Valenca GP, Nunhez JR (2013). Effect of immobilized cells in calcium alginate beads in alcoholic fermentation. AMB Express 3(1):31.
Eckert CT, Frigo EP, Albrecht LP, Albrecht AJP, Christ D, Santos WG, Berkembrock E, Egewarth VA (2018). Maize ethanol production in Brazil: characteristics and perspectives. Renewable and Sustainable Energy Reviews 82(3):3907-3912.
FAOSTAT (2017). http://www.fao.org/faostat/en/#(accessed//.05.17).
Hansen AC, Zhang Q, Lyne PWL (2005). Ethanol diesel fuel blends – a review. Bioresource Technology 96(3):277-285.
Hussain A, Kangwa M, Abo-Elwafa AG, Fernandez-Lahore M (2015). Influence of operational parameters on the fluid-side mass transfer resistance observed in a packed bed bioreactor. AMB Express 5:25.
Lareo M, Ferrari MD, Guigou M, Fajardo L, Larnaudie V, Ramirez MB, Garreiro JM (2013). Evaluation of sweet potato for fuel bioethanol production: hydrolysis and fermentation. Springer plus 2:493.
Lee KH, Choi IS, Kim YG, Yang DJ, Bae HJ (2011). Enhanced production of bioethanol and ultrastructure characteristics of reused *Saccharomyces cerevisiae* immobilized calcium alginate beads. Bioresource Technology 102(17):8191-8198.
Nwuche CO, Murata Y, Nweze JE, Ndubuisi IA, Omae H, Saito U, Ogbonna JC (2018). Bioethanol production under multiple stress condition by a new acid and temperature tolerant *Saccharomyces cerevisiae* strain LC 269108 isolated from rotten fruits. Process Biochemistry 67:105-112.
Ogbonna JC, Amano Y, Kazuo N (1989). Elucidation of optimum conditions for immobilization of viable cells by using calcium alginate. Journal of Fermentation and Bioengineering 67(2):92-96.
Ogbonna JC, Matsumura M, Kataeka H (1991). Effective oxygenation of immobilized cells through reduction in bead diameter. Process Biochemistry 26(2):109-121.
Oyeagu U, Nwuche CO, Ogbonna CN, Ogbonna JC (2018). Addition of fillers to sodium alginate solution improves stability and immobilization capacity of the resulting calcium alginate beads. Iranian Journal of Biotechnology 16(1):67-73.
Perego C, Peratello S (1999). Experimental methods in catalytic kinetics. Catalysis Today 52(2-3):133-145.
Puligundla P, Poludasu RM, Rai JK, Obulan VSR (2011). Repeated batch ethanolic fermentation of very high gravity medium by immobilized *Saccharomyces cerevisiae*. Annals of Microbiology 61(4):863-869.
Rattanapan A, Limtong S, Phisalaphong M (2011). Ethanol production by repeated batch and continuous fermentations of blackstrap molasses using immobilized yeast cells on the shell silk cocoons. Applied Energy 88(12):4400-4404.
Sarkar N, Ghosh SK, Bannerjee S, Aikat K (2012). Bioethanol production from agricultural wastes: an overview. Renewable Energy 37(1):19-27.
Siqueira PF, Krap SG, Carvalho JC, Sturm W, Rodrigues - Leon JA, Tholozan JL, Singhania RR, Pandey A, Soccol CR (2008). Production of bioethanol from soybean molasses by *Saccharomyces cerevisiae* at laboratory, pilot and industrial scales. Bioresource Technology 99(17):8156-8163.
Standard Methods for the Examination of Water and Waste Water (2005). 21st edition, American Public Health Association (APHA), American Water Works Association (AWWA) and Water Environment Federation (WEF), Washington, D.C., USA.
Watanabe I, Miyata N, Ando A, Shiroma R, Tokuyasu K, Nakamura T (2012). Ethanol production by repeated batch simultaneous saccharification and fermentation (SSF) of alkali-treated rice straw using immobilized *Saccharomyces cerevisiae* cells. Bioresource Technology 123:695-698.
Yao W, Wu X, Zhu J, Sun B, Zhang YY, Miller C (2011). Bacterial cellulose membrane – a new support carrier for yeast immobilization for ethanol fermentation. Process Biochemistry 46(10):2054-2058.

Vol. 18(21), pp. 452-461, 22 May, 2019
DOI: 10.5897/AJB2019.16768
Article Number: D6FE16B60980
ISSN: 1684-5315

http://www.academicjournals.org/AJB

ACADEMIC JOURNALS
expand your knowledge

African Journal of Biotechnology

Full Length Research Paper

Quantitative trait loci (QTL) mapping for intermittent drought tolerance in BRB 191 × SEQ 1027 Andean Intra-gene cross recombinant inbred line population of common bean (*Phaseolus vulgaris* L.).

M. Nabateregga[1*], C. Mukankusi[2], B. Raatz[3], R. Edema[1], S. Nkalubo[4] and B. M. E. Alladassi[1]

[1]College of Agricultural and Environmental Science, Department of Agricultural Production, Makerere University, P. O. Box 7062 Kampala, Uganda.
[2]International Centre for Tropical Agriculture (CIAT), P. O. Box 6247 Kampala, Uganda.
[3]CIAT-International Centre for Tropical Agriculture, Cali, Colombia.
[4]National Crops Resources Research Institute, Namulonge, P. O. Box 7084, Kampala, Uganda.

Received 11 February 2019; Accepted 8 April, 2019

Drought is a major constraint of common bean (*Phaseolus vulgaris* L.) production in Uganda where irrigation for the crop is very uncommon. This study aimed to identify quantitative trait loci (QTLs) underlying drought tolerance in 128 F5 RILs derived from an Andean intra-gene cross between drought-tolerant SEQ 1027 and BRB 191. Eighteen traits were evaluated under drought stress and non-stress conditions in the field for 2 years and in the greenhouse for 1 year, respectively. A linkage map spanning 486.29 cM was constructed using 53 single nucleotide polymorphic markers (SNP) markers obtained from the KASP genotyping assay. Eleven consistent QTLs were detected on five linkage groups at a threshold of Logarithm of Odds (LOD) ≥ 3.0. Four QTLs were constitutive, seven were adaptive and were associated with 100 seed weight, grain yield, chlorophyll content, harvest index, dry weight of leaf and stem biomass and yield production efficiency. The QTL associated with a 100 seed weight (*sw3.1^{BS}*) was the most consistent with the highest percentage of variation explained (21%). Co-localization of five drought-related factors QTLs was detected on pv10 suggesting pleiotropic effects on this chromosome. Identification of molecular markers closely linked to the QTLs identified in this study will facilitate marker assisted breeding for drought tolerance.

Key words: Common bean, drought tolerance, single nucleotide polymorphism, quantitative trait loci.

INTRODUCTION

Common bean is consumed by large numbers of the poor in Africa (Singh and Munoz, 1999). The crop provides protein, complex carbohydrates, and valuable micronutrients for more than 300 million people in the tropics and is a staple crop for over 200 million people in sub-Saharan Africa (Akibode, 2011). The crop therefore

*Corresponding author. E-mail: mnabateregga@gmail.com.

plays an important role in mitigating protein malnutrition and micronutrient deficiencies in regions where their effects are prevalent. Furthermore, epidemiological studies also have shown that a regular diet with beans brings great benefits to health due to the fact that it reduces the risk of developing cancer, diabetes and heart disease (Guajardo-Flores et al., 2013). The importance of common bean will increase in the future especially in tropical Africa where the demand is even likely to increase as the human population increases (Wortmann, 2006; Baudoin and Mergeai, 2001). In East Africa, beans are primarily grown by the smallholder farmers, especially women, for home consumption, while any excess production is sold at the market (Spence, 2006).

Drought has been recognized as one of the most important bean production constraint affecting 60% of bean production in drought prone areas worldwide. On-farm yields of beans in East Africa and Uganda in this case, have remained stagnant (0.5 to 0.6 Mt ha^{-1}) (Sibiko, 2012; Kalyebara and Buruchara, 2008), a case attributed to a multitude of biotic and abiotic constraints affecting bean production under low input systems. Rainfall in the country is highly variable and unpredictable in most parts of bean production, and yet most of the country's agriculture is rain-fed; this has made major dry bean yield losses inevitable (NEMA, 2001; Okonya et al., 2013). Effects of drought in major agricultural areas are expected to increase due to climate change, which will negatively affect crop yields and food security (McClean et al., 2011). It should also be noted that the bean is very sensitive to both soil and environmental fluctuations which has made breeding for drought tolerance in the crop especially difficult. As a result, only a few breeding schemes have been successful in improving the efficiency of genetic enhancement of the common bean for drought tolerance.

Significant research efforts have been made, particularly over the past two to three decades, to improve common bean adaptation to drought and, as such, key drought genetic resources have also been identified. Genetic variation for most traits associated with drought tolerance has shown a quantitative inheritance (Asfaw et al., 2012; Blair et al., 2012). However, the underlying genetic basis of most of these traits is yet to be understood. Also, quantitative trait loci (QTL) underlying drought tolerance in the common bean have been discovered over the past two decades (Rao et al., 2006), although marker assisted selection using markers linked to these QTL is still uncommon. In the future, effective use of genomic tools will be efficient with a better understanding of the physiology of drought response and drought resistance mechanisms. Furthermore, Mesoamerican beans are the most widely grown beans around the world and are found in areas where drought stress is on the increase (Blair et al., 2012). As such, most QTL studies in drought tolerance have been carried out using Mesoamerican and intergene populations. Thus, more studies using Andean derived crosses are needed to explore additional diversity for drought resistance QTL alleles, and to analyze the effect of genetic backgrounds on the QTL alleles that have already been identified.

In common bean, molecular and protein markers were used to construct the first genetic linkage maps (Nodari et al., 1993). Amplified fragment length polymorphisms (AFLP), simple sequence repeats (SSR), resistance gene analogs (RGA) and single nucleotide polymorphic markers (SNP) have since been added to increase the density of existing maps. SNP markers are expected to provide the opportunity to produce high density maps enabling high precision QTL mapping in common bean. Limited drought studies in common bean have been conducted in the region and as a result marker-assisted breeding for drought tolerance has not yet been fully implemented. This could be due to the variability of drought stress, limited capacity for phenotyping, absence of high-throughput marker systems as well as the lack of knowledge of the genetics of drought resistance mechanisms. QTL analysis for drought tolerance across a range of environmental conditions using a dense map would improve the identification of QTL associated with broad adaptation to drought stress in common bean.

The objective of this study was to identify QTL underlying drought tolerance in the Andean cross of (BRB 191×SEQ 1027) RIL population. More studies in this field would greatly contribute to breeding programs through marker-assisted selection and broaden our understanding of the mechanisms behind drought tolerance, a key to averting production losses due to drought. In the near future, specific breeding strategies have to be developed to address all kinds of drought.

MATERIALS AND METHODS

The mapping population

An intra-gene pool RIL population consisting of 128 lines was derived from a cross between BRB 191 and SEQ1027, two Andean cultivars with bush growth habit. BRB 191 is the source of the *bc3* gene that confers resistance to Bean Common Mosaic Virus (BCMV) and its necrotic strain Bean Common Mosaic Necrosis Virus (BCMNV) while SEQ 1027 is a drought tolerant cultivar developed at CIAT (CIAT, 2008). The population was developed at CIAT, Cali by artificial hybridization to create an initial F_1 hybrid followed by single seed descent (SSD) from the F_2 up to the F_5 generation. CIAT-Cali lies at an altitude of about 965 m with latitude 3°30'N and longitude of 76°30'W. The average temperatures are 24.3°C ranging from 18.8 to 28.4°C. Average rain fall is 896 mm and soils are fine silty, mixed, isohyperthermic Aquic Hapludoll. The population was evaluated along with eight experimental checks using incomplete block alpha-lattice design replicated twice. The evaluation was carried out under field conditions for 2 years and greenhouse conditions for 1 year at the National Agricultural Research Laboratories (NARL), Kawanda. The checks included Diacol calima, DAB 494, SEQ 1003, SCR 9, DAB 441, NABE 4, CAL 96 and BAT 477. Each experiment consisted of two water regimes treatment, non-stress (NS) where the plants were irrigated when there was no rain, and drought stress (DS) where there was no irrigation as described by Nabateregga et al. (2018).

In the greenhouse, soil was collected from a bean growing field site and mixed with sand to form a soil: sand mixture in a 2:1 proportion by weight (Polania et al., 2012). Sand was included to induce drought treatment faster than with soil alone. The soil was fertilized with adequate level of nutrients using NPK. The soil-sand mixture was poured into plastic and transparent 2 L pots of 15 cm diameter and 10 cm height with 3 small holes at the bottom to allow drainage. The pots were filled to the brim with the soil-sand mixture. Seeds were sterilized with a solution of 5% calcium hypochlorite for 5 min to reduce exposure to bean disease pests and placed on germination paper under ambient conditions for 2 days before planting (Makunde, 2013).

Phenotypic data collection and analysis

During the phenotypic evaluation, 18 phenological, morphological and physiological traits were measured (Nabateregga et al., 2018). Drought intensity index (DII) was computed in each given environment as: 1-(Xs/Xi) (Fischer and Maurer, 1978); where Xs is the grand mean yield of all genotypes grown under drought stress and Xi is the grand mean yield of all genotypes grown under optimum conditions.

Histograms were drawn to observe the distribution of the genotypes means averaged across the two years under each water regime treatment. Pearson correlation analysis was also conducted to determine the linear relationship between the phenotypic traits evaluated under the two water treatments conditions herein presented as heat-map. The phenotypic data analysis was carried out using the R open source statistical software version 3.5.1.

Genetic mapping and QTL analysis

A bulk leaf tissue sample of three F5 plants collected from seedlings of each cultivar in the population was used for DNA extraction. The population, along with the parents, was genotyped using the BARCBean6K-3 SNP array which contained a total of 5398 bead-types (Michigan State University, 2012) at KBiosciences. A linkage map was constructed using QTL ICIMapping software (Version 4.0, www.isbreeding.net; Jiankang et al., 2014). This was done after data from SNP genotyping of the population was manually inspected in an excel sheet to eliminate SNPs with no call or those which were monomorphic between parents. Besides, SNPs markers with distorted segregation were also checked and excluded from the map construction using Chi-square goodness-of-fit test at 5% significance level. The map was generated using the maximum likelihood mapping algorithm of QTL ICIM 4.0 and linkage groups were determined at a Logarithm of Odds (LOD) score of 3.0 and a maximum distance of 50 cM using the Haldane units (Lander et al., 1987). QTL analysis was conducted using composite interval mapping (CIM) in the ICI-Mapping software (Zhang et al., 2012) with 1 cM walk speed, a 0.001 PIN and 3.0 LOD significant threshold. The marker within the QTL peak with the highest phenotypic variation explained (PVE) and level of probability ($P \leq 0.01$) were used to define the genomic position of the QTL. The analysis was done using the genotype means first for individual environments and then combined (average over the two years) in combined years analysis. To be reported, a QTL had to be detected in more than one environment and identified QTL were named according to the 'Guidelines for common bean QTL nomenclature' (Miklas and Porch, 2010). This consisted of combining a three-letter code for the trait with the linkage group and the order of the QTL for the given trait on each linkage group. For example, $SY1.1^{BS}$ represents the first QTL for seed yield on chromosome Pv01 in the BRB/SEQ RIL population. Single environment analysis model was preferred to the multi-environment mixed model approach in order to detect repeatability, consistency and therefore usefulness of the QTL.

RESULTS

Drought stress effects on select phenotypic traits and correlation among traits

Drought stress was the most severe during the field trial of 2014 with a drought intensity index (DII) of 0.78 followed by the greenhouse trial (DII of 0.58) while the 2015 field trial had the least index of 0.42. Overall, the drought stress affected the performance of the RILs for the various traits studied as shown by the distribution on the histogram (Figure 1). The RILs performed generally better under no stress (NS) conditions than drought stress (DS) for most of the traits; except for pod partitioning and harvest indices where the population had a relatively similar performance under both DS and ND (Figure 1). This was mainly noted for traits such as grain yield where under DS, none of the lines produced more than 300 kg/plot while under NS, about 40% of the RILs had a yield greater than 400 kg/plot. It was however noted that, under DS conditions, some lines performed equally good or better than the best performing ones under NS which is indicative of their resilience to water stress. This was the case for traits like pod partitioning index (PPI), yield production efficiency and chlorophyll content (Figure 1).

A perfect positive correlation was observed among yield production efficiency (YPE), pod partitioning index (PPI) and harvest index (HI) on one hand and between seed and pod biomass on the other hand (Figure 2). On the contrary, a very strong negative correlation was observed between pod harvest index (PHI) and pod wall biomass proportion (PWBP).

With a specific focus on correlation between yield and other traits, 100 seed weight and yield production efficiency (YPE) had moderate and low positive correlations with yield under DS and NS, respectively (Figure 2). Harvest and pod partitioning indices (HI and PPI) had a positive correlation with yield which was moderate under NS but weak under DS unlike pod harvest index (PHI) which showed an opposite pattern with a weak correlation under NS but moderate under DS. In general, moderately high positive correlations were observed between the dry weight of various biomass components and yield under both DS and NS (Figure 2). Seed biomass at harvest (SD.H) had the highest correlation under DS. Canopy temperature showed moderate negative correlation with yield under NS and none under DS. Regardless of the water stress conditions, no correlation was observed between yield and stem biomass reduction (SBR) and chlorophyll content (SPAD) (Figure 2).

Identification of quantitative trait loci for drought tolerance

The binning tool in ICIM software (version 4.0) removed

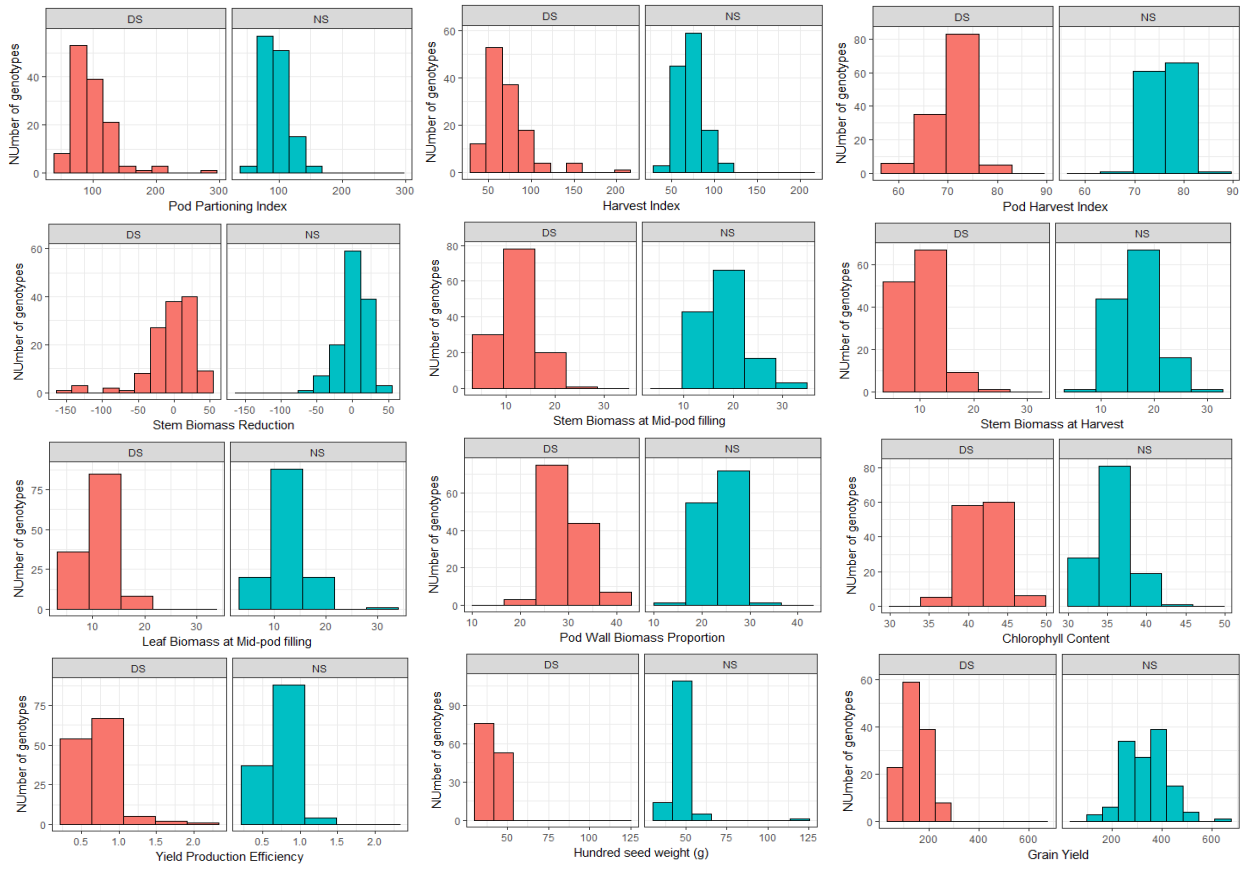

Figure 1. Distribution of BRB 191 × SEQ 1027 recombinant inbred lines' means for select traits studied means under drought stress and non-stress conditions at Kawanda in 2014 and 2015.

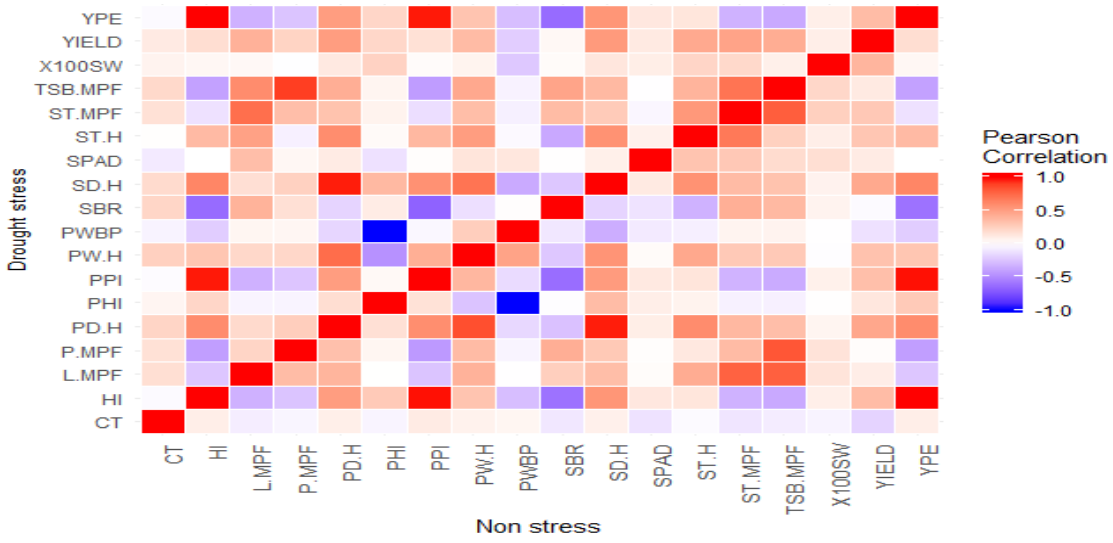

Figure 2. Heat map of Pearson correlation among traits studied under drought stress (below diagonal) and non-stress (above diagonal) conditions in 2014 and 2015 at Kawanda. YPE: Yield production efficiency; 100SW: hundred seed weight; TSB.MPF: total shoot biomass at mid-pod filling; ST.MPF: stem biomass at mid-pod filling; ST.H: stem biomass at harvest; SPAD: chlorophyll content; SD.H: seed biomass at harvest; SBR: stem biomass reduction; PWBP: pod wall biomass proportion; PW.H: pod wall biomass at harvest; PPI: pod partitioning index; PHI: pod harvest index; PD.H: pod biomass at harvest; P.MPF: pod biomass at mid-pod filling; L.MPF: leaf biomass at mid-pod filling; HI: harvest index; CT: canopy temperature.

Table 1. Anchor groups of the linkage map with the number of flanking markers and distance for each chromosome.

Chr ID	Anchor group	Number of SNP markers	Length (cM)
Pv01	1	3	41.221
Pv02	2	2	32.93
Pv03	3	3	30.198
Pv04	4	6	92.545
Pv05	5	1	0
Pv06	6	1	0
Pv07	7	1	0
Pv08	8	3	61.546
Pv09	9	11	107.418
Pv10	10	19	81.861
Pv11	11	3	38.571
Whole Genome		53	486.29

Chr ID: Chromosome identity.

redundant markers and those with high missing rates to produce 53 markers that were used to construct the linkage map of 11 anchor groups. Map saturation was low with three (pv5, pv6 and pv7) of the genetic groups carrying only one marker (Table 1). Linkage groups pv10 and pv9 had the highest number of markers (19 and 11 markers, respectively). The BRB 191/SEQ 1027 map spanned 486.29 cM with the 9th anchor group having the longest span of 107.418 cM (Table 1). The interval between markers for the 11 anchor groups ranged from 0.19 to 82.39 cM with an average distance of 12.03 cM between markers. The 11 linkage groups represented 40.52% limited genome coverage of common bean that has an estimated total size of 1200 cM.

Inclusive composite interval mapping (ICIM) identified eleven major QTLs (LOD ≥ 3.00, P<0.05) from all experiments. All major QTL were located on 5 linkage groups, namely pv01, pv03, pv04 and pv08 and pv10 (Table 2); linkage group 10 (pv10) had the highest number of major QTLs (6) while pv08, pv04 and pv01 had only one. A major 'hot spot' was identified on pv10 where six QTLs clustered between position 40 and 60 cM (Figure 3). Consistent QTLs were detected for grain yield on pv03 and pv10 (*gy3.1*^{bs} and *gy10.1*^{bs}). Both QTLs were adaptive in nature being detected under non-stress conditions of 2015 and combined environments and they originated from BRB 191. The percentage of variation explained (PVE) for *gy10.1*^{bs} was equal in both environments (9%) with comparable additive effects while *gy3.1*^{bs} explained 4.9 to 7.2% percentage increase in seed yield on pv03. There was co-localization between the QTLs *sw3.1*^{bs} related with seed weight and *gy3.1*^{bs} related with grain yield on pv03 at 94.2 cM. However, the latter was detected under non-stress conditions of 2014 while the former under drought stress in 2014.

The QTL associated with 100 seed weight (*sw3.1*^{bs}) was the most consistent; appearing in five environments namely drought stress (DS) conditions of 2014 and 2015, non-stress (NS) conditions of 2015 and combined environments of DS and NS. This constitutive QTL was detected on pv03 between 92.7 and 94.2 cM and expressed its highest additive effects under combined non-stress conditions (Table 2). Other consistent QTL detected in this study included those associated with chlorophyll content (*scmr8.1*^{bs} and *scmr10.1*^{bs}) on pv08 and pv10, harvest index (*hi10.1*^{bs} and *hi10.2*^{bs}) on pv10, dry weight of stem biomass at mid-pod filling (*stmpf1.1*^{bs}) on pv01 and dry weight of leaf biomass at mid-pod filling (*lmpf4.1*^{bs}) on pv04.

Both *scmr8.1*^{bs} and *scmr10.1*^{bs} originated from the female parent (BRB 191), however, the former was adaptive in nature (detected under drought stress conditions only) while the latter was constitutive being detected under both drought stress and non-stress in greenhouse. *scmr8.1*^{bs} had a PVE ranging from 21.3 to 22% while *scmr10.1*^{bs} increased chlorophyll content by a percentage that ranged from 1.7 to 16.7% (Table 2). The two QTLs for harvest index *hi10.1*^{bs} and *hi10.2*^{bs} were both consistent with the former being adaptive to non-stress conditions of 2015 and combined environments. On the other hand, *hi10.2*^{bs} was constitutive in nature appearing under drought stress conditions of 2014 and combined non-stress environments (Table 2).

Coming to dry mass components, two QTLs were detected namely *stmpf1.1*^{bs} associated with stem dry mass at MPF on linkage group pv01 and *lmpf4.1*^{bs} associated with leaf dry mass at MPF on pv04. *stmpf1.1*^{bs} was adaptive to drought stress conditions and was detected between 26.5 to 56 cM explaining 10.6 to 11.9% increase in stem dry mass at MPF on pv01. Similarly, *lmpf4.1*^{bs} was adaptive in nature, being detected under non-stress conditions. It originated from BRB 191 and was detected between 0 and 2.5 cM on pv04; explaining 3.7 to 6.5% increases in leaf dry mass.

Table 2. Major QTL identified by ICIM from phenotypic data from field and greenhouse evaluation at Kawanda.

Trait of association	Environment	Treatment	Chr	QTL	QTL peak position (cM)	QTL interval (cM)	LOD	PVE (%)	Additive effect
100 Seed weight	Field	Combined_DS	3	*sw3.1*^{bs}	94.2	93.7-94.2	4.6	21.2	1.5
	Field	Combined_NS	3		94.2	92.7-94.2	4.3	0.2	2.0
	Field	DS14	3		94.2	92.7-94.2	3.8	12.3	1.9
	Field	DS15	3		94.2	92.7-94.2	3.2	15.1	1.4
	Field	NS15	3		94.2	92.7-94.2	3.7	1.1	1.3
Chlorophyll content	Field	Combined_DS	8	*scmr8.1*^{bs}	71.9	71.9-72.4	6.5	21.3	-0.9
	Field	DS14	8		71.9	71.9-72.4	6.1	22	-1.5
	Greenhouse	DS_GH	10	*scmr10.1*^{bs}	58.3	57.8-58.8	27.2	16.7	-2.0
	Greenhouse	NS_GH	10		58.3	57.8-59.8	5	1.7	-0.9
Grain yield	Field	Combined_NS	3	*gy3.1*^{bs}	89.2	78.7-94.2	4.7	4.8	-32.8
	Field	NS15	3		94.2	92.7-94.2	3.2	7.2	-38.1
	Field	Combined_NS	10	*gy10.1*^{bs}	52.3	49.8-57.8	9.9	9	-45.2
	Field	NS15	10		57.3	50.8-57.8	4.1	9	-42.8
Harvest index	Field	Combined_NS	10	*hi10.1*^{bs}	41.3	19.8-45.8	4.2	1.3	5.6
	Field	NS15	10		42.3	39.8-45.8	4.3	7.4	9.1
	Field	Combined_NS	10	*hi10.2*^{bs}	62.3	60.8-63.8	3	0.8	-4.4
	Field	DS14	10		62.3	60.8-62.8	11.8	5.7	22.1
Leaf Biomass at MPF	Field	Combined_NS	4	*lmpf4.1*^{bs}	0.0	0-2.5	3.2	3.7	-1.0
	Field	NS15	4		0.0	0-2.5	3.5	6.5	-1.4
Stem Biomass at MPF	Field	DS14	1	*stmpf1.1*^{bs}	42.0	26.5-56	3.4	10.6	-1.6
	Field	Combined_DS	1		50.0	29.5-56	3.5	11.9	-1.7
Yield Production Efficiency	Field	Combined_NS	10	*ype10.1*^{bs}	41.3	19.8-45.8	4.2	1.3	0.1
	Field	NS15	10		42.3	39.8-45.8	4.3	7.4	0.1
	Field	Combined_NS	10	*ype10.2*^{bs}	62.3	60.8-63.8	3	0.8	0.0
	Field	DS14	10		62.3	60.8-62.8	11.8	5.7	0.2

Chr: Chromosome, Position: marker position in cM on the chromosome, LOD: logarithm of odds, PVE (%): phenotypic variation explained, DS: drought stress, NS: non-stress.

DISCUSSION

The labor intensity involved in phenotyping for drought tolerance has made marker assisted breeding (MAB) a desirable tool in drought tolerance breeding programs. This study aimed at identifying QTLs that can provide markers that could potentially be used in MAB. The efficiency of QTL mapping is highly dependent on marker density (Mukeshimana et al., 2014; Perez-Vega et al., 2010). The genetic map constructed in this study had a size of 486.29 cM developed using 53 anchored polymorphic SNPs markers of the KASP genotyping assay. The successful construction of a genetic map using an Andean intragene cross population was critical given that Andean beans are widely grown in Uganda where drought stress is on the increase (Kalyebara and Buruchara, 2008; Miller, 2014).

Several studies have identified drought related QTLs (Asfaw et al., 2012; Mukeshimana et al., 2014); however, stable expression of these QTL across different stress environments is still rare (Trapp et al., 2015). This is because quantitative traits are highly dependent on

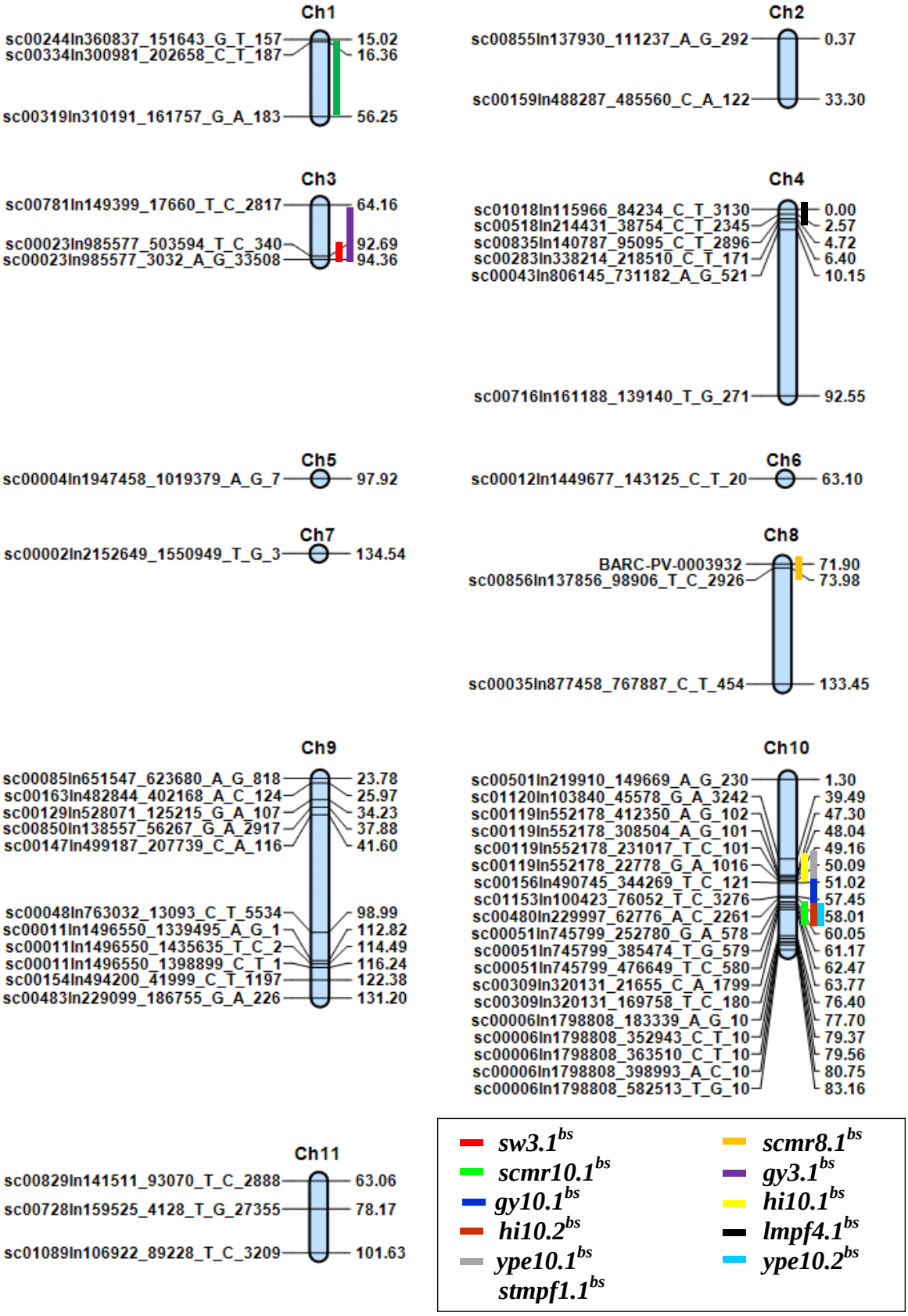

Figure 3. Linkage map of the BRB 191 × SEQ 1027 population and the QTLs identified Constructed using QTL ICI-Mapping software version 4.0 (Wang et al., 2014).

environmental conditions and therefore variations in drought stress (in terms of timing, duration and intensity) as well as other abiotic and biotic factors can influence expression of quantitative genetic factors (Blum, 2011). Furthermore, the exclusive use of bi-parental mapping populations which enable only two alleles for any one gene to be evaluated (Xu and Crouch, 2008) also reduces the probability of detecting QTL consistently. In this study, QTLs were detected under both DS and NS conditions in 2014 as well as in 2015. About 70% of the QTLs identified were adaptive to either DS or NS while the other 30% were constitutive suggesting a high likelihood of consistent expression of the latter. Besides, half of the QTLs identified in this study originated from the male parent SEQ 1027 and this genotype was reported in previous studies as a superior Andean genotype for drought adaptation (CIAT, 2008; Asfaw, 2011) and as such the cultivar has been used in many breeding programs (Makunde, 2007).

The QTL analysis showed that the traits 100 seed weight, chlorophyll content, grain yield harvest index, leaf and stem dry mass and yield production efficiency are important to consider for selection for drought tolerance. Two genomic regions were found to be associated with grain yield on linkage groups pv03 and pv10 and these findings are consistent with previous research. Trapp et al. (2015), used Buster × Roza RIL population and detected a QTL on pv10 associated with yield (SY10.1) located at 39.9 cM in close vicinity of *gy10.1*^{bs} reported in this study at 49.3 cM. In another study on pinto bean population, Hoyos-Villegas et al. (2015) reported three QTLs associated with seed yield of which one was on Pv03 in proximity with *gy3.1*^{bs} of this study. Similar to the present results, Blair et al. (2012) also discovered yield-associated QTL on pv03 and pv10 adaptive to non-stress and drought stress conditions, respectively. However, unlike Yld10.1 in his study, *gy10.1*^{bs} is adaptive to non-stress condition though they both had relatively equal additive effects of 56.1 and 51.4, respectively. Wright and Kelly (2011) also identified two QTL for seed yield on pv10 and on Pv03 using a RIL population of black bean parents Jaguar and 115M. Blair et al. (2006) also found two small-effects QTL on Pv03 from two-season data using a population derived from a cross between ICA Cerinza and G24404 (red bean). Miklas et al. (2007) reported a QTL for yield on Pv03 in two locations in different years in a RIL population from the cross between Aztec and ND-88-106-04. There are variations in findings between this study and previous studies; however, this could arise from differences in environment, marker technologies and populations used. Nevertheless, there is strong indication that pv03 and pv10 carry genetic factors conditioning seed yield.

A QTL for 100 seed weight was exclusively mapped in one region on pv03 (*sw3.1*^{bs}) and originated from SEQ 1027 parent. It was the most consistent in the study and was detected under both DS and NS conditions, which implied that genes on this chromosome might have a constitutive mechanism that conditions seed weight. Consistency in expression of *sw3.1*^{bs} suggests higher heritability and stability; highlighting the importance of seed weight in marker assisted breeding (Collins et al., 2008). It explained up to 21.2% of increase in seed weight under DS conditions and also co-localized with seed yield QTL *gy3.1*^{bs}. Negative linkages of seed weight and seed yield potential in common bean has been and is still problematic in bean breeding (Beaver and Osorno, 2009); however, positive correlation observed in this study provide opportunity for simultaneous selection for these two traits in Andean intra-gene crosses. Previous studies have also identified QTL for seed weight on pv03. In a study aimed at identifying QTL for root architecture traits correlated with phosphorus acquisition, Beebe et al. (2006) detected Swf3.1 associated with SW using a cross between Andean G19833 and Mesoamerican DOR 364. Mukeshimana et al. (2014) also identified an important constitutive QTL for seed weight on pv03 (SW3.1SC) that explained 8 to 16% of the phenotypic variation. Similar to *sw3.1*^{bs}, SW3.1SC was associated with yield under NS conditions. The seed weight QTL *sw3.1*^{bs} also confirms results from various previous studies that mapped seed weight on Pv03 using RFLP and RAPD markers (Nodari et al., 1993; Park et al., 2000). Most recently, Sandhu et al. (2018) used 80,398 SNP markers on a cross between black bean lines BK004-001 and H68-4 and mapped QTL for seed weight on three linkage groups including pv03.

Repeatability of QTL across environments is an indicator of stability and increased heritability which improves efficiency of traits in marker-assisted breeding. Selecting for drought tolerance using constitutive QTL such as *sw3.1*^{bs} in common bean under drought stress would favorably increase yield under non-stress conditions as well. Another important trait with a constitutive QTL was harvest index on pv10 (*hi10.2*^{bs}) that explained 6% of the phenotypic variation. The second QTL for harvest index, *hi10.1*^{bs} was adaptive to non-stress conditions. Using composite interval mapping, Asfaw et al. (2012) also reported QTLs for harvest index of which one was mapped on pv10 under non-stress conditions with a percentage variation of 0.12 to 0.23% similar to *hi10.1*^{bs}. The stability of expression of *hi10.2*^{bs} QTL under both drought stress and non-stress conditions is an indicator that marker assisted breeding using markers tightly linked to HI could possibly increase drought tolerance across a wide range of environments. Several studies have shown improved remobilization of photosynthate to grain to be an important mechanism under drought stress (Asfaw et al., 2012; Mukeshimana et al., 2014; Trapp et al., 2015); however, pyramiding different tolerance mechanisms will help develop a more sustainable drought adaptation in common bean.

In this study, we have also identified two QTLs associated with the dry weight of leaf and stem biomass (*stmpf1.1*^{bs} and *lmpf4.1*^{bs}) on pv01 and pv04,

respectively. Similar findings were reported by Briñez et al. (2017) who detected SBF1.1^{AS}, a QTL associated with stem biomass, on linkage group 1. This QTL had the same percentage variation explained as *stmpf1.1*^{bs} (PVE =10.26%) highlighting the important role of this genomic region in the expression of drought tolerance mechanism. Repinski et al (2012) also mapped the PvTFL1y gene that controls stem dry mass and ease of mechanized harvest on pv01 (linkage group 1) in common bean, and this further supports the present findings.

While in this study consistent QTLs associated with chlorophyll content were detected on pv08 and pv10 (*scmr8.1*^{bs} and *scmr10.1*^{bs}), on pv01, pv06 and pv11; these were inconsistently compared to the ones identified in this study that appeared in more than one environment. However, it should be noted that the percentage variations for chlorophyll content detected in the Briñez et al. (2017) study had higher percentage variations explained, ranging from 11.2 to 32.9% compared to the 1.7 to 21% reported in this present study. Briñez et al. (2017) used SSRs and SNP markers to map QTLs in a SEA 5 × AND 277 common bean cross. Asfaw et al. (2012) identified 13 QTL associated with chlorophyll content of which three were detected on pv08 and pv10 as found in this study. Similar to this study, these QTL detected on pv10 were constitutive like *scmr10.1*^{bs} while those found on pv08 were adaptive in nature to drought stress conditions like *scmr8.1*^{bs}. However, it should be noted that high chlorophyll content does not necessarily translate to higher yields. Some have reported that thick, small, and dark green leaves under drought might be less photosynthetically active because of closed stomata despite high chlorophyll content (Asfaw et al., 2012), and as such SPAD readings and QTL for this trait may be less useful under severe drought stress compared with moderate stress.

Finally, one of the highlights in this study was co-localization of QTL on pv10. Co-localization of drought-related factors on pv10 was an indication of pleiotropic effects on the chromosome (Aastveit and Aastveit, 1993) and confirmed the complexity of seed yield under drought stress, a phenomenon determined by many physiological processes throughout crop growth. Clustering of several related factors could also have been because these traits are physiologically related and may have a common biochemical pathway. Co-localization of QTL for correlated variables such as phenology, yield, and yield components on the same chromosome has also been reported in other studies (Mukeshimana et al., 2014; Trapp et al., 2015; Briñez et al., 2017).

In conclusion, the present study identified 11 important constitutive and adaptive drought tolerance-associated QTLs in the BRB 191 × SEQ 1027 RIL population. These results agree with previous studies which mapped drought related QTLs in similar chromosome regions thus demonstrating the merits of QTL mapping using SNP technologies as a precision tool in genetic studies. New regions containing novel QTLs were also identified in this study for drought related traits such as stomatal conductance, biomass accumulation and photosynthate remobilization. These results will help for fine mapping candidate genes controlling these traits hence an important tool that can be used for selection. The knowledge about these QTLs will also help foster marker-assisted selection in common bean breeding programs using SEQ 1027 as source of drought tolerance. In view of the complexity of seed yield under drought stress, and the inconsistency in the expression of trait associated QTL across environments and mapping populations, selection using a combination of drought related traits would produce more stable and high yielding genotypes.

CONFLICT OF INTERESTS

The authors have not declared any conflict of interests.

ACKNOWLEDGEMENTS

The authors thank Dr. R. Bodo and International Centre for Tropical Agriculture (CIAT) for providing the mapping population used in this study. CIAT also funded the research through the Tropical Legumes II project (TLII).

REFERENCES

Aastveit AH, Aastveit K (1993). Effects of genotype-environment interactions on genetic correlations. Theoretical and Applied Genetics 86(8):1007-1013.

Akibode CS (2011). Trends in the production, trade, and consumption of food-legume crops in sub-Saharan Africa. (No. 1097-2016-88694).

Asfaw A, Blair MW, Struik, PC (2012). Multi-environment quantitative trait loci analysis for photosynthate acquisition, accumulation, and remobilization traits in common bean under drought stress. G3-Genes Genomes Genetics 2(5):579-595.

Baudoin JP, Mergeai G (2001). Grain Legumes in Crop production in Tropical Africa. BNARDA (2003). Annual Report 25:313-317.

Beaver JS, Osorno JM (2009). Achievements and limitations of contemporary common bean breeding using conventional and molecular approaches. Euphytica 168(2):145-175.

Beebe SE, Rojas-Pierce M, Yan X, Blair MW, Pedraza F, Munoz F, Tohme J, Lynch JP (2006). Quantitative trait loci for root architecture traits correlated with phosphorus acquisition in common bean. Crop Science 46(1):413-423.

Blair MW, Galeano CH, Tovar E, Torres MCM, Castrillón AV, Beebe SE, Rao IM (2012). Development of a Mesoamerican intra-genepool genetic map for quantitative trait loci detection in a drought tolerant × susceptible common bean (*Phaseolus vulgaris* L.) cross. Molecular Breeding 29(1):71-88.

Blair MW, Giraldo MC, Buendia HF, Tovar E, Duque MC, Beebe SE (2006). Microsatellite marker diversity in common bean (*Phaseolus vulgaris* L.). Theoretical and Applied Genetics 113(1):100-109.

Blum A (2011). Plant water relations, plant stress and plant production. In Plant breeding for water-limited environments. Springer, New York, NY. pp. 11-52.

Briñez B, Perseguini JMKC, Rosa JS, Bassi D, Gonçalves JGR, Almeida C, Valdisser PAMR (2017). Mapping QTLs for drought lerance in a SEA 5 x AND 277 common bean cross with SSRs and SNP markers. Genetics and Molecular Biology 40(4):813-823.

CIAT (2008). Annual report 2008. Outcome line SBA-1. Improved beans for the developing world.

Collins NC, Tardieu F, Tuberosa R (2008). Quantitative trait loci and crop performance under abiotic stress: where do we stand? Plant Physiology 147(2):469-486.
Guajardo-Flores D, Serna-Saldívar SO, Gutiérrez-Uribe JA (2013). Evaluation of the antioxidant and anti-proliferative activities of extracted saponins and flavonols from germinated black beans (*Phaseolus vulgaris* L.). Food chemistry 141(2):1497-1503.
Kalyebara R, Buruchara RA (2008). The impact of improved bush bean varieties in Uganda. Centro Internacional de Agricultura Tropical (CIAT), Kampala, UG. 2 p. (Highlights: CIAT in Africa no. 43).
Lander ES, Green P, Abrahamson J, Barlow A, Daly MJ, Lincoln SE, Newburg L (1987). MAPMAKER: An interactive computer package for constructing primary genetic linkage maps of experimental and natural populations. Genomics 1(2):174-181.
Makunde G (2013). Quantification of genetic diversity for drought adaptation in a reference collection of common bean (*Phaseolus vulgaris* L.). University of The Free State, Bloemfontein, South Africa.
Makunde GS (2007). Combining ability for drought tolerance in common bean. (University of Zambia, Lusaka, Zambia).
McClean PE, Burridge J, Beebe S, Rao IM, Porch TG (2011). Crop improvement in the era of climate change: an integrated, multi-disciplinary approach for common bean (Phaseolus vulgaris). Functional Plant Biology 38(12):927-933.
Miklas PN, Porch T (2010). Guidelines for common bean QTL nomenclature. Annual Report Bean Improvement Cooperation 53:202-204.
Miklas PN, Larsen KM, Terpstra KA, Hauf DC, Grafton KF, Kelly JD (2007). QTL analysis of ICA Bunsi-derived resistance to white mold in a pinto× navy bean cross. Crop science 47(1):174-179.
Miller LC (2014). Feed the Future Innovation Lab for Collaborative Research on Nutrition-Asia Heifer International-Annual Report-Year 4 (Doctoral dissertation, Department of Child Study & Human Development, Tufts University).
Mukeshimana G, Butare L, Cregan PB, Blair MW, Kelly JD (2014). Quantitative trait loci associated with drought tolerance in common bean. Crop Science 54(3):923-938.
Nabateregga M, Mukankusi C, Raatz B, Edema R, Nkalubo S, Alladassi BME (2018). Effect of intermittent drought on phenotypic traits of F5 RIL Andean intra-gene cross population (BRB 191 x SEQ 1027) of common bean. African Crop Science Journal 26(4):555-573.
National Environment Management Authority (NEMA) (2001). District Population Densities and Protected Areas, NEMA, Kampala, Uganda.
Nodari RO, Tsai SM, Guzman P, Gilbertson RL, Gepts P (1993). Toward an integrated linkage map of common bean, mapping genetic factors controlling host-bacteria interactions. Genetics 134(1):341-350.
Okonya JS, Syndikus K, Kroschel J (2013). Farmers' perception of and coping strategies to climate change: evidence from six Agro-ecological zones of Uganda. Journal of Agricultural Science 5(8):252-262.
Park SO, Coyne DP, Jung G, Skroch PW, Arnaud-Santana E, Steadman JR, Nienhuis J (2000). Mapping of QTL for seed size and shape traits in common bean. Journal of the American Society for Horticultural Science 125(4):466-475.
Rao IM, Beebe S, Polania J, Grajales MA, Garcia R (2006). Differences in drought resistance of advanced lines developed for the last 3 decades. Project IP-1: Bean improvement for the tropics: CIAT Annual Report 2-6.
Repinski SL, Kwak M, Gepts P (2012). The common bean growth habit gene PvTFL1y is a functional homolog of Arabidopsis TFL1. Theoretical and Applied Genetics 124(8):1539-1547.
Sandhu KS, You FM, Conner RL, Balasubramanian PM, Hou A (2018). Genetic analysis and QTL mapping of the seed hardness trait in a black common bean (*Phaseolus vulgaris* L) recombinant inbred line (RIL) population. Molecular breeding 38(3):34.
Sibiko KW (2012). Determinants of common bean productivity and efficiency: A case of smallholder farmers in Eastern Uganda. (No. 634-2016-41491).
Singh SP, Munoz CG (1999). Resistance to common bacterial blight among Phaseolus species and common bean improvement. Crop Science 39(1):80-89.
Spence N (2006). Bean root rot disease management in Uganda. (DFID project ref, R8478, NR Int Code ZA0689): Final technical report, International Development Team, Central Science Laboratory (DEFRA).
Trapp JJ, Urrea CA, Cregan PB, Miklas PN (2015). Quantitative trait loci for yield under multiple stress and drought conditions in a dry bean population. Crop Science 55(4):1596-1607.
Wang X, Pang Y, Zhang J, Zhang Q, Tao Y, Feng B, Li Z (2014). Genetic background effects on QTL and QTL× environment interaction for yield and its component traits as revealed by reciprocal introgression lines in rice. The Crop Journal 2(6):345-357.
Wortmann CS (2006). *Phaseolus vulgaris* L (common bean). Record from PROTA4U. Bring M. and Belay, G. PROTA (Plant Resource of Tropical Africa). Wageningen, Netherlands
Wright EM, Kelly JD (2011). Mapping QTL for seed yield and canning quality following processing of black bean (*Phaseolus vulgaris* L.). Euphytica, 179(3):471-484.
Xu Y, Crouch JH (2008). Marker-assisted selection in plant breeding: From publications to practice. Crop Science 48(2):391-407.
Zhang L, Li H, Wang J (2012). The statistical power of inclusive composite interval mapping in detecting digenic epistasis showing common F2 segregation ratios. Journal of integrative Plant Biology 54(4):270-279.

Vol. 18(21), pp. 462-471, 22 May, 2019
DOI: 10.5897/AJB2019.16762
Article Number: 1B85DD461005
ISSN: 1684-5315

http://www.academicjournals.org/AJB

African Journal of Biotechnology

Full Length Research Paper

Chemical study of *Peganum harmala* seeds

Isabela Araujo e Amariz*, Jacyara Pereira da Silva, Emanuella Chiara Valença Pereira, Nathália Andrezza Carvalho de Souza, José Marcos Teixeira de Alencar Filho, Renan Nunes Pereira, Ana Paula de Oliveira and Larissa Araújo Rolim

Center for Drug, Food and Medicine Analysis, Federal University of São Francisco Valley - Petrolina (PE), Brazil.

Received 5 February 2019; Accepted 12 April, 2019

Peganum harmala **belongs to the family Zygophyllaceae and is popularly known as "Arruda of Syria". It presents a broad therapeutic potential, highlighting the anti inflammatory, anticancer, analgesic, antiseptic and antibacterial activities. It is used in the preparation of religious rituals beverages with effects on the central nervous system as an inhibitor of the enzyme monoaminoxidase, whose action is due to the presence of harmonic alkaloids of the β–carbolines group, with harmine and harmaline being the most found in** ***P. harmala*** **seeds. The objective of this study was to evaluate the chemical and pharmacognostic characteristics of** ***P. harmala*** **seeds with the aid of gas chromatography coupled to mass spectrometry. Pharmacognostic characterization was performed following the 5th edition of the Brazilian Pharmacopoeia. Scanning electron microscopy coupled to X-ray dispersive energy spectroscopy was performed for the seeds elemental identification. The compounds present in the species were identified by gas chromatography coupled to mass spectrometry. Phytochemical evaluation demonstrated the major secondary metabolites. The scanning electron microscopy coupled to X-ray dispersive energy spectroscopy analysis showed the morphology of the surface and interior of the seeds, as well as the atomic chemical analysis of the structures. By gas chromatography coupled to mass spectrometry, the chemical profile of** ***P. harmala*** **seeds was identified and the β–carbolines (harmaline and harmine) were identified, which are compounds of great pharmacological importance for the species. Therefore, it is concluded that this study is of great contribution to the plant material standardization that will serve as the basis for the future development of a pharmaceutical product.**

Key words: Arruda of Syria, characterization, gas chromatography, β-carbolines, *Peganum harmala*.

INTRODUCTION

The use of natural products for therapeutic purposes comes from the beginning of the civilizations. A large portion of the world's population, especially from developing countries, makes use of herbal medicines relying on them for the cure, prevention and treatment of diseases. In addition, it is a source of bioactive compounds, which contributes to the development of new therapeutic strategies (Firmo et al., 2018).

Peganum harmala popularly known as "Syrian rust", belongs to the family Zygophyllaceae, being well adapted

*Corresponding author. E-mail: Isabela.amariz26@gmail.com. Tel: +55 87 99993-4030.

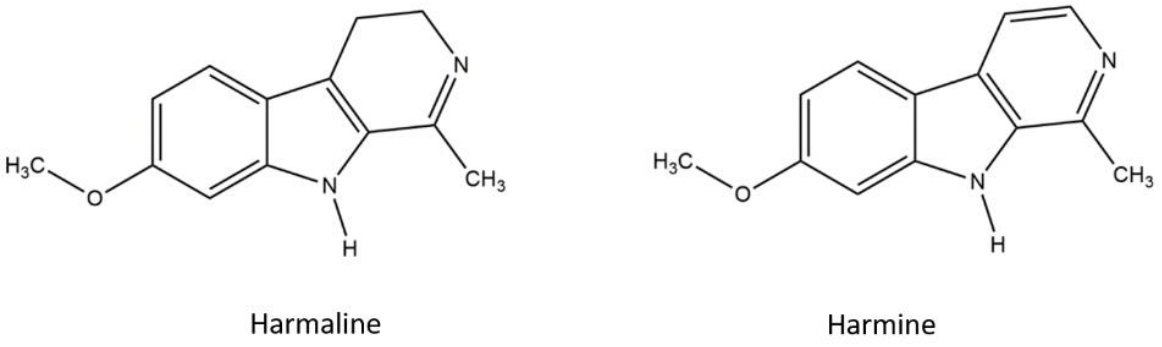

Figure 1. Chemical structure of β–carbolines: Harmaline and Harmine, respectively.

to the climate of dry regions mainly found in North Africa, Middle East, India and Mongolia (Herraiz et al., 2010). This species has several therapeutic purposes, mainly highlighting the neuropharmacological, antidepressive and hallucinogenic activities. These activities come from β-carbolines, a group of harmonic alkaloids found in a variety of plants (Sassoui et al., 2005). In the seeds of *P. harmala* the most commonly β-carbolines (Figure 1) found are: harmine, harmaline and tetrahydroharmine (Rodrigues, 2013; Muller, 2006).

The β-carbolines action is similar to monoamine oxidase (iMAO) inhibitor drugs, which act by deactivating this enzyme responsible for the monoamines degradation (serotonin and catecholamines), and thus act by regulating and / or increasing their levels in the synaptic cleft (Herraiz et al., 2010; Moloudizargari et al., 2013).

In view of these pharmacological actions, *P. harmala* is an important source of β-carbolines and it can be used as a vegetable raw material for the development of phytotherapeutic drugs or phytomedicines containing these active substances. Therefore, the objective of this study was to evaluate the chemical and pharmacognostic characteristics of *P. harmala* seeds with the help of gas chromatography coupled to mass spectrometry (GC-MS).

MATERIALS AND METHODS

Collection of plant material

The *P. harmala* seeds were purchased in local commerce in the city of Petrolina-PE, in July 2016 and were identified based on herbarium specimens in Herbarium Alexandre Leal Costa – ALCB located in the Department of Botany of the Institute of Biology of the Federal University of Bahia (UFBA), under the code ALCB 12384 (Code: ALCB014643, Type of record: preserved specimen).

Solvents

The solvents used were: Ultra purified water (Milli–Q), Absolute Ethyl Alcohol P.A (Synth®), Acetonitrile (Merck®), Formic acid (Dinâmica®), Methanol (Merck®), Acetate of ethyl (HPLC grade).

Obtaining powder and preparing extracts

The seeds of *P. harmala* were oven dried in circulating air at 40°C for 96 h and then pulverized in a knife mill. Then, the dried and pulverized seeds were subjected to thorought maceration with absolute ethyl alcohol -99.5% PA (ethanol) with renewal of the extracting liquid every 72 h. The solutions were filtered and concentrated on a rotary evaporator (50°C) to obtain the crude ethanolic extract of *P. harmala* (EtOHB of *P. harmala*).

Pharmacognostic characterization of vegetable drug

P. harmala seed powder was used to perform the physical-chemical tests: loss determination by desiccation, the powders granulometry, total ashes, acid insoluble ash, sulfated ash, foam index and extractable substances through alcohol as described and recommended in the Brazilian Pharmacopoeia 5th Edition (Brazil, 2010; Luis et al., 2015; Kaskoos, 2014). For the determination of the powders granulometry, a set of five previously weighed sieves with mesh diameters of 500, 425, 250, 180 and 150 µm and a collector were selected. Physical-chemical tests were performed in triplicate and the results were expressed as mean ± standard deviation.

Electronic scan microscopy (SEM) of the seeds of *P. harmala*

The sample was prepared on double carbon tape contained in copper and nonmetallized stub. SEM analyzes of *P. harmala* seeds were obtained by JOEL® scanning electron microscope, model JSM–5900, coupled to a dispersive energy analyzer (EDS) using increases of 300 and 750 times.

Preliminary phytochemical assessment

The phytochemical evaluation of the crude ethanolic extract of *P. harmala* (EtOHB of *P. harmala*) was carried out using silica gel chromatography plates with aluminum support, applied with micropipette and eluted in different solvent systems, according to Wagner and Bladt (1996) to show the main groups of secondary metabolites.

Analysis by gas chromatography coupled to mass spectrometry (GC–MS)

The gas chromatography coupled to mass spectrometry (GC-MS)

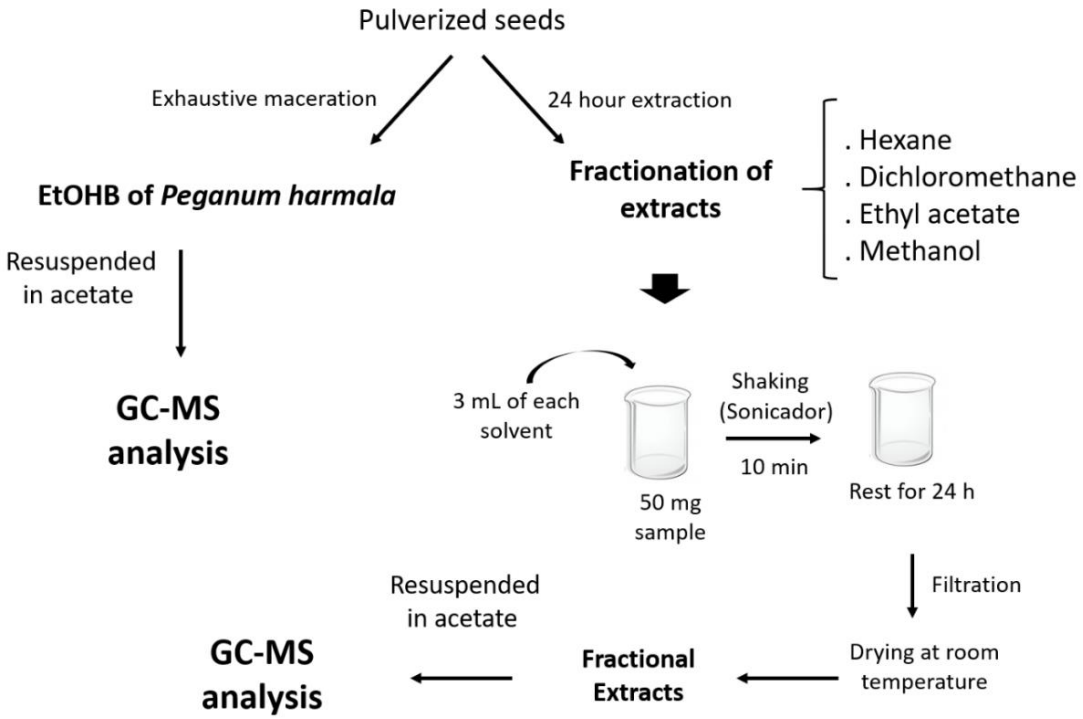

Figure 2. Schematic representation of *P. harmala* extracts by GC-MS.

was used to evaluate the chemical profile of the plant species from the analysis of EtOHB of *P. harmala* and the analysis of the fractionated extracts based on the increasing polarity of the solvents: hexane, dichloromethane, ethyl acetate and methanol, respectively.

P. harmala seeds were divided into two groups: Group A obtained from whole seeds; and Group B obtained from seeds divided in half. An amount of 50 mg was weighed, and then 3 ml of each solvent (in increasing order of polarity) was added and brought to sonicator shaking for 10 min with each solvent. It was allowed to stand for 24 h. After this time, the sample was filtered and added to the next solvent. The extract was dried at room temperature (25°C) by air circulation. This process was repeated for each new solvent and performed in triplicate. EtOHB of *P. harmala* was obtained according to the methodology described for obtaining and preparing the extracts described above. For the samples analysis resuspension was necessary in ethyl acetate (Grade High Performance Liquid Chromatography (HPLC)) in concentration of 10 mg/ml and then analysis on a gas chromatograph was performed coupled to a Shimadzu® mass spectrometer (QP-2010) and coupled to a self injector (AOC 20i) was used employing the following chromatographic conditions: RESTEK® RTX–5MS column (30.0 mm × 0.25 mm × 0.25 mm) using helium gas (99.99%) transported with a constant flow of 1.4 mL / min, sample injection volume of 1.0 µL, split mode with ratio 5 (split 1: 4 discard), injector temperature 260°C; electron impact mode at 70 eV; ion source temperature of 250°C. The oven temperature was programmed to 80°C (isothermal for 3 min), increasing from 5°C/min to 285°C (isothermal for 15 min) and 10°C/min to 320°C (isothermal for 20 min). A linear hydrocarbon mixture (C 9 H 20 – C 40 H 82) was injected under the same conditions as the samples under analysis, and the compunds identification was by comparison of the mass spectra obtained with the spectra presented by the SHIMADZU® database (GCMS Solution) (Wiley 7lib and NIST08lib) (Carvalho et al., 2014). The compound was considered as identified when it presented similarity index greater than or equal to 90% (Figure 2).

RESULTS AND DISCUSSION

Pharmacognostic characterization of vegetable drug

Weight loss

To determine the weight loss of the seeds of *P. harmala*, the gravimetric method described in the Brazilian Pharmacopoeia (2010) (Brasil, 2010) was used. The results presented a moisture content of 7.41 ± 0.02 in the seeds of *P. harmala*, this value is close to previous studies in which the results were 6.94 ± 1.05 (Kaskoos, 2014).

Granulometric determination of the powders

After the sieving process, it was observed that the largest amount of *P. harmala* powder was retained in the 850 µm mesh, as shown in the histogram of Figure 3A. The determination of the average particle size was carried out by calculating the percentage of the passage fraction and the fraction of powder retained in each of the sieves. The results obtained in graphical representation showed that the average particle size of *P. harmala* represented in the graph was 473 µm (Figure 3B), being classified as coarse

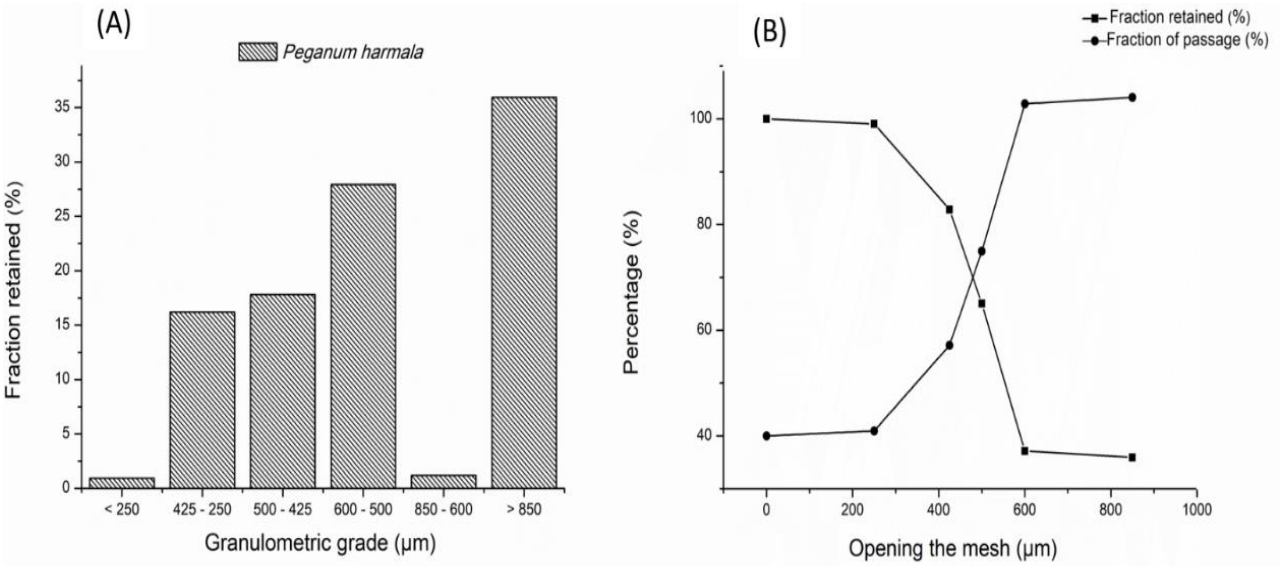

Figure 3. (A) Histogram of granulometric distribution of *P. harmala* seeds powder, (B) Graphical determination of the particle size of the obtained powder of *P. harmala*.

powder according to the Brazilian Pharmacopoeia (2010) (Brasil, 2010).

Determination of total ashes, acid insoluble ash and sulphated ash

The results of total ashes, acid insoluble ash and sulfated ashes of the plant drugs are shown in Table 1. The Brazilian Pharmacopoeia recommends the maximum values of 8 % for total ashes and 1.5 % for acid insoluble ashes. As it is possible to see in Table 1, the results obtained are in disagreement with this recommendation (Brasil, 2010). Comparing the results found with the studies by Kaskoos (2014), it was observed that the total ash content is very high (7.51 ± 1.16), whereas for the acid insoluble ash content the value was 1.56 ± 0.61 (Kaskoos, 2014). As the analyzes performed above have the purpose of performing the sample characterization, the results of this study indicate that this species has higher values than those commonly found. Such a characteristic condition of this plant drug may be related to changes in the conditions of cultivation, processing, transport and/or harvesting.

These quality parameters are important, being possible to evaluate the amount of contaminants present in the sample, such as sand, stone, bad processing and others. These results, when found in the sample, lead to changes in values (Couto et al., 2009). The high content of sulphated ash in the *P. harmala* sample may be indicative of the high amount of crystalline content in the seeds of this species. In plants, the crystalline mineral inclusions contribute to the ashes increase, mainly influencing the values of sulfated ash (Tengku et al., 2013).

Determination of foam index

The presence of saponins in the plant drug can be determined from the foam index test. This is due to the ability of saponins to form persistent and abundant foams in aqueous solution because of their amphiphilic nature, where sapogenin (lipophilic part) interacts with apolar compounds and sugar chains, interact with polar substances (Podolak et al., 2010).

According to the results of the performed test, after 15 min of analysis the foam formation was less than 1 cm in height, being thus the obtained index less than 100 demonstrating absence of saponins in *P. harmala.* Studies of Kaskoos (2014) also evidenced the absence of saponins when using the same test described by the Brazilian Pharmacopoeia (Kaskoos, 2014). Some studies report the presence of saponins in this species, but by using this test it was not possible to identify the same. Preliminary phytochemical evaluation was performed using the Wagner and Bladt (1996) methodology to verify the presence of secondary metabolites of the species and consequently the presence of saponins.

Determination of substances withdrawn by alcohol

For the determination of the content of extractable substances in ethanol the result obtained was 35.72 ± 0.52%. The extractive content provides primordial information on the substances that can be extracted with a certain solvent, and consequently indicate the yield of the different types of extraction used in the plant material technological transformation (Couto et al., 2009; Simões et al., 2017).

Table 1. Determination of ash content in *P. harmala* seeds

Species	Total ashes	Insoluble sshes in acid	Sulphated ashes
P. harmala	10.12 ± 1.55%	9.41± 1.29%	12.08 ± 0.15 %

Table 2. Phytochemical profile of the crude ethanolic extract of *P. harmala.*

Chemical class	EtOHB - PH
Alkaloids	++
Anthocyanins	+++
Aglycone Anthraquinone	+
Flavonoids	+++
Cumarines	+
Anthracene Derivatives	+
Lignans	-
Mono, sesqui and diterpenes	++
Napthtoquinones	-
Saponins	+++
Condensed tannins	++
Hydrolysable tannins	++
Triterpenes and steroids	+++
Xanthines	-

Preliminary phytochemical assessment

The results of the phytochemical analysis of EtOHB of *P. harmala* are shown in Table 2. The phytochemical analysis of EtOHB of *P. harmala* demonstrated the presence of alkaloids, saponins, coumarins, anthraquinones, anthocyanins, anthracene derivatives, monoterpenes, sesquiterpenes, diterpenes, triterpenes and tannins (condensed and hydrolysable). The result was negative for the presence of lignans, naphthoquinones and xanthines. These results are presented in Table 2.

In the genus *Peganum* compounds are found such as, alkaloids, triterpenoids, anthraquinones, flavonoids, carbohydrates, amino acids, volatile oils, sterols, vitamins among others. The alkaloids β-carbolines and quinazoline are characteristic of this genus and some of them are bioactive constituents exerting some type of therapeutic effect. Some examples of β-carbolines are harmalol, harmaline, harmine, harmana, tetrahydroharmine (Li et al., 2017).

Electronic scan microscopy (SEM) of the seeds of *P. harmala*

Scanning electron microscopy (SEM) coupled with X-ray dispersive energy (EDS) spectroscopy, was carried out to provide a quantitative chemical characterization of *P. harmala* seeds (Figure 4), as well as to aid in taxonomic identification. For better visualization, the seeds were distributed in order to visualize the seeds interior morphology. From these analyzes it is possible to observe the seed anatomical structure, observing the three main structures: tegument endosperm and embryo (Figure 4), whose functions are protection, nutrition and development, respectively.

The EDS evaluates the characteristic X-rays that are generated from the beam-electron interaction, informing the elements that compose the sample in the form of spectra (histograms) and it is also possible to identify the individual elements. Currently, most scanning electron microscopes are coupled to a dispersive energy spectrometer (Cruz et al., 2006). The elements identification present in the seeds of *P. harmala*, among them, carbon (C), oxygen (O), phosphorus (P), potassium (K), sulfur (S), chlorine (Cl), calcium, is shown in Figure 5. The presence of macronutrients in plants is important both for the primary metabolism and for the production of different secondary metabolites (Gobbo-Neto and Lopes, 2007). When the plant undergoes nutritional stress, it is common to increase the secondary metabolites concentration.

Analysis by gas chromatography coupled to mass spectrometry (GC-MS)

The GC-MS analysis aimed to evaluate the chemical profile of *P. harmala* seeds by observing the main

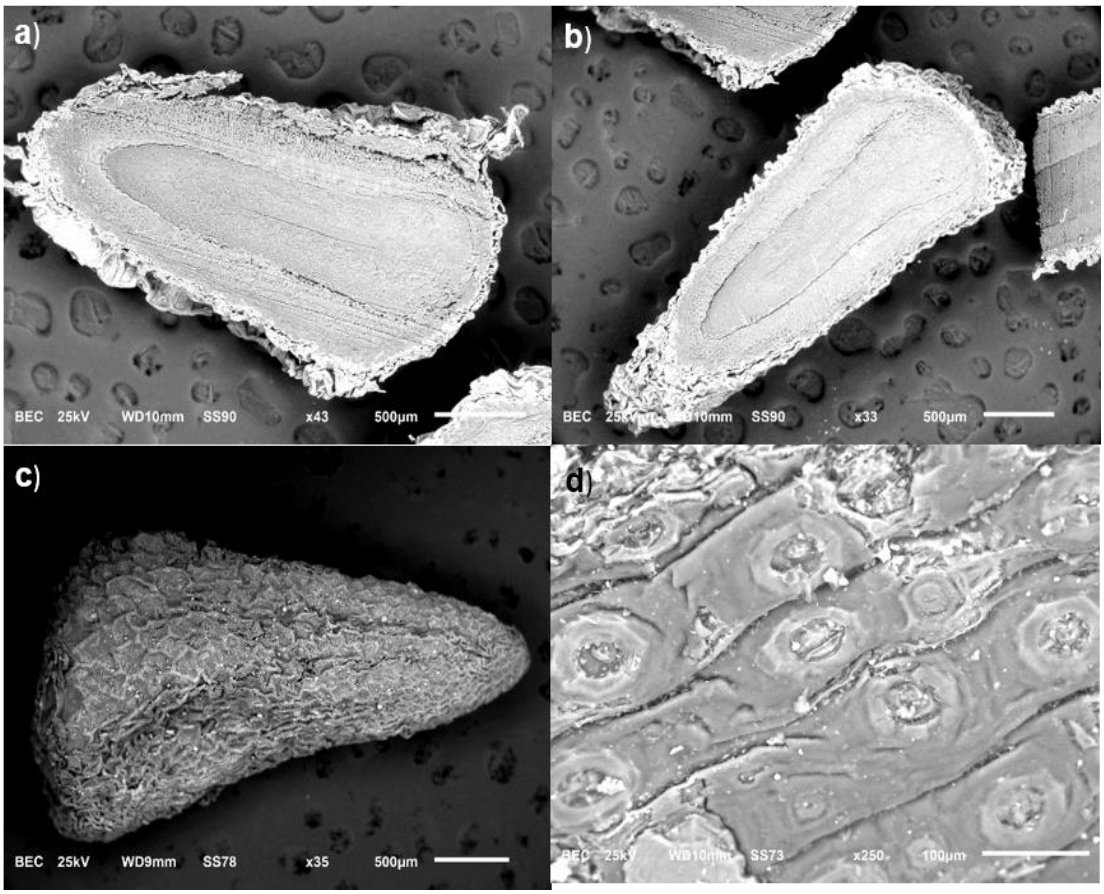

Figure 4. Photomicrographs of *P. harmala* seeds. (a) and (b) internal structure by longitudinal section; (c) and d) external structure evidencing the seed surface.

chemical constituents present. The identification occurs through molecular mass and the fragmentation profile generated by mass spectrometry, being in this technique the compounds separated from the volatization capacity of each one (Pavia et al., 2010).

In the chromatogram obtained after the GC-MS analysis of EtOHB of *P. harmala* (Figure 6), the presence of 18 peaks was observed, two β-carbolines were identified: peak 12 at harmaline (abundance of 0.29%-retention time 33.1 min) and peak 13 at harmine (abundance 7.34%-retention time 34 min). The identified compounds are shown in Table 3.

According to studies by OTT (1994), it was verified that harmine is found in greater quantity, in relation to harmaline in the seeds of *P. harmala*, which can justify the more effective action concerning iMAO by Harmine (Santos, 2007).

According to the studies of Tavares (2014), the determination of the harmaline and harmine alkaloids by gas phase chromatography allows better separation and identification of a more selective form. Further, according to their studies, the identification ions for harmaline are m / z 170 in / z 198, while for harmine, m / z 169 are in z / z 198 (Tavares, 2014), confirming what is demonstrated in the mass spectra of Figures 7 and 8, respectively. The results found corroborate with the data described in the literature and confirm the presence of the two compounds (harmaline and harmine), in the seeds of *P. harmala*.

In addition to these compounds, other hydrocarbons and their derivatives and fatty acids were identified, corresponding in the average identification of 80% of the chemical composition of the sample.

In the analysis performed by solvent partitioning, the objective was to show the chemical profile of *P. harmala* based on the affinity for the solvent used. The four extractions obtained with solvents in increasing order of polarity were analyzed: hexane, chloroform, ethyl acetate and methanol. From this, it was possible to visualize the chemical profile and the identification of the compounds present in greater quantity in the respective extracts. The compounds identification was performed according to the comparison of the similarity index of the compounds found in the software library. The two groups of the analysed seeds were: group A (whole seeds) and group B (seeds shaved in the middle), in order to evaluate if the extractive process would be more efficient with the seeds

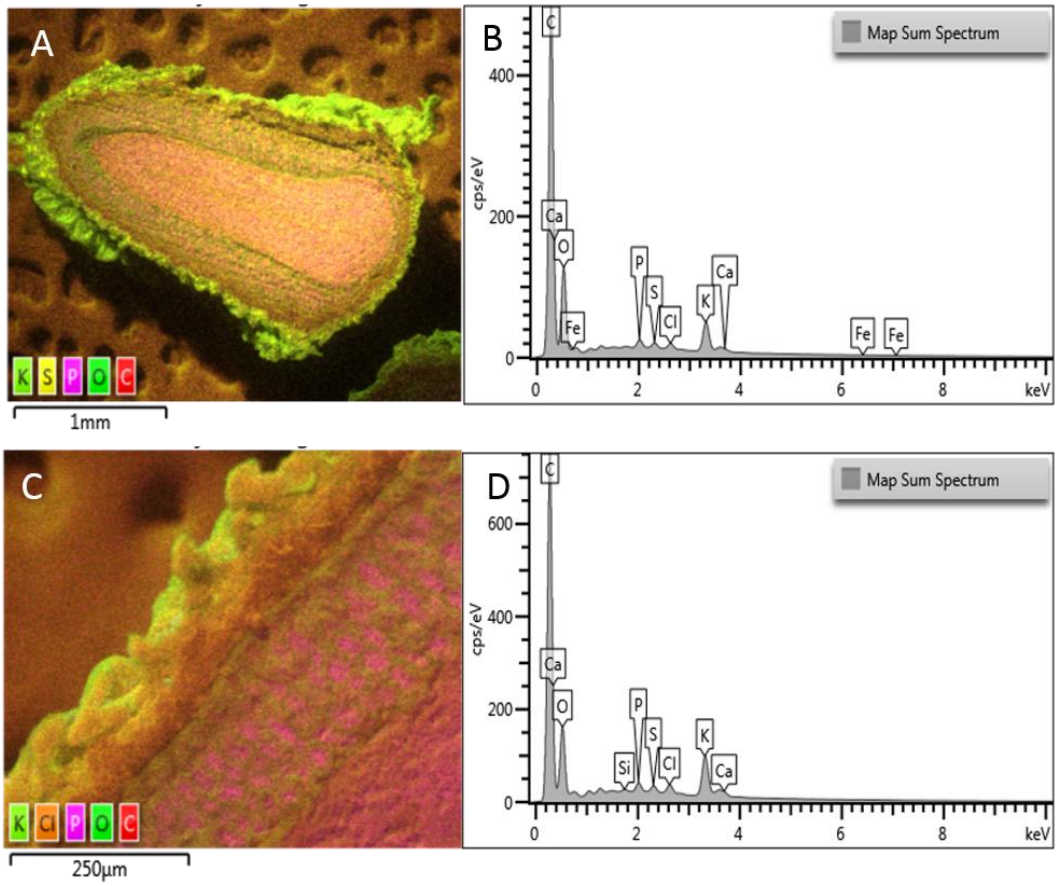

Figure 5. Photomicrographs A and C, respectively; and EDS B and D, corresponding to the seeds of *P. harmala*.

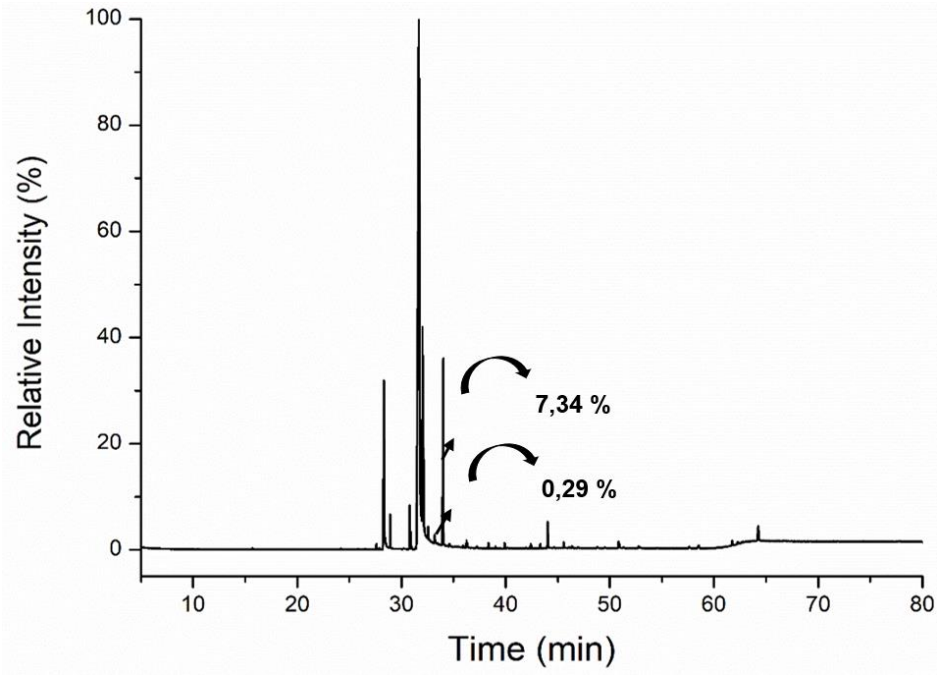

Figure 6. Chromatogram obtained after GC-MS analysis of EtOHB of *P. harmala* seeds.

Table 3. Identification of chemical constituents of crude ethanolic extract of *P. harmala* seeds by CG–MS. ND: not detected.

Retention time	Area	Area (%)	Name	m/z
28.315	17161385	8.48	Hexadecanoic acid	256
30.793	2388497	1.21	9,12-Octadecadienoic acid, methyl ester	294
30.901	983298	0.48	9-Octadecenoic acid (Z)-, methyl ester	278
31.667	93971890	46.44	Oleic acid, methyl ester	280
31.737	35831922	17.71	Octadec-9-enoic acid	282
32.019	14696352	7.26	Linoleic acid ethyl ester	279
32.112	7363111	3.63	Ethyl Oleate	310
32.216	2645169	1.31	ND	ND
32.355	706059	0.34	ND	ND
32.435	1006238	0.51	ND	ND
32.560	1745026	0.86	Octadecanoic acid, ethyl ester, Ethyl stearate	312
32.675	598424	0.29	ND	ND
33.193	637104	0.31	Harmaline	213 / 215
34.007	15845150	7.83	Harmine	212
36.249	440816	0.21	ND	ND
39.890	486937	0.24	ND	
44.028	1911462	0.95	Delta-tocopherol	402
45.578	446436	0.22	ND	ND
50.856	889410	0.44	ND	ND
58.526	470374	0.23	ND	ND
61.746	470308	0.23	ND	ND
64.249	1645318	0.82	ND	ND

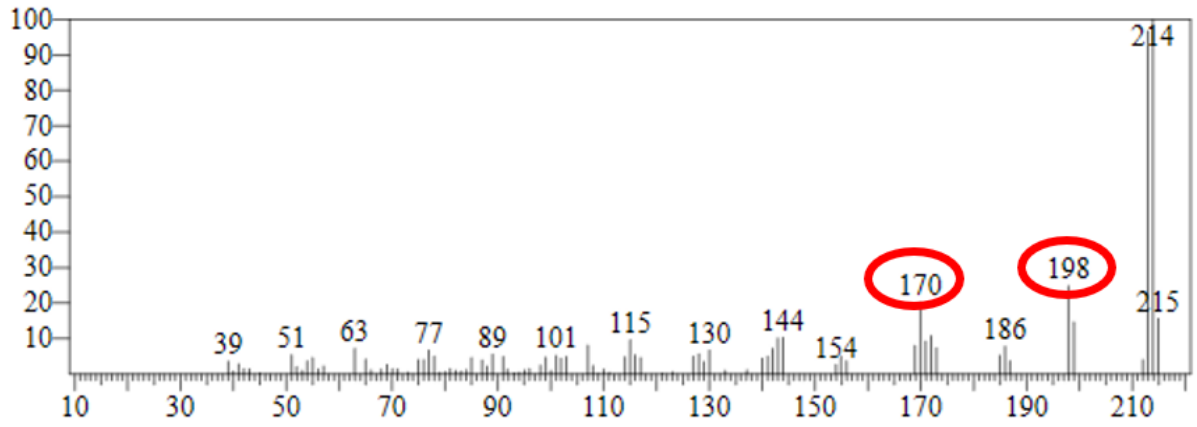

Figure 7. Mass spectrum obtained for harmaline in the EtOHB of *P. harmala*.

shaved in the middle or if it would be possible to extract the β-carbolines with the whole seeds, which facilitates the samples processing.

In the analysis of the seeds of group A with the solvent hexane, the presence of 17 peaks was observed, only one peak (retention time 42.0 min) was identified as the pentacosan hydrocarbon, it was not possible to identify the β-carbolines harmaline and harmine. The extraction with the solvents dichloromethane and ethyl acetate allowed the harmine compound identification, in which in the extraction with the dichloromethane harmine represented 81.0% of the chemical composition of the sample and in the extraction with ethyl acetate represented 91.04% of the sample chemical composition. In the analysis of the extraction with methanol the presence of 22 peaks was detected, among them it was possible to identify the presence of β-carbolines harmine (27.5%) and harmaline (1%), hydrocarbons and their derivatives, fatty acids, besides triterpenes betulin (11%) and lupenone (3.5%). The seeds analysis of group B with

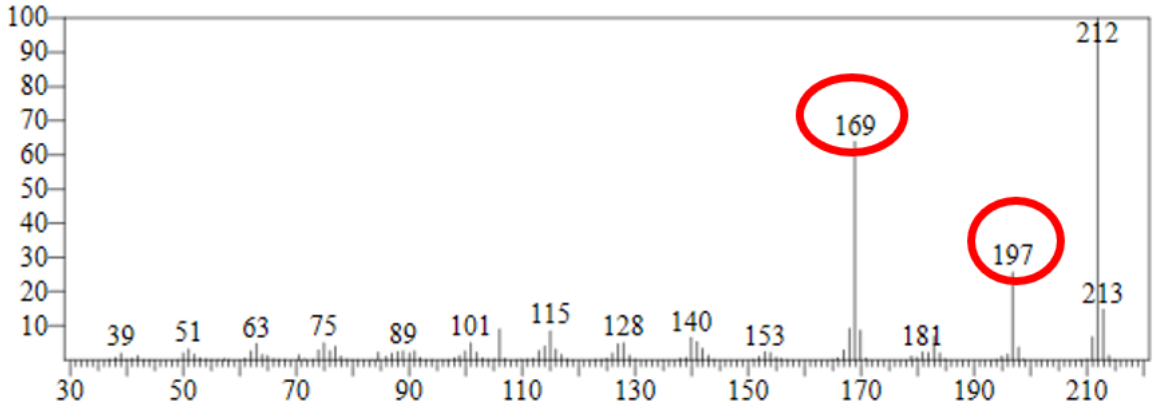

Figure 8. Mass spectrum obtained for harmine in the EtOHB of *P. harmala*.

Table 4. Quantitative relationship of harmaline and harmine composition present in the fractionated extracts of *P. harmala*.

		Hexane		Dichloromethane		Ethyl acetate		Methanol	
		A	**B**	**A**	**B**	**A**	**B**	**A**	**B**
Harmaline	RT 32.0 min	ND	ND	ND	ND	ND	ND	1.0%	ND
	m/z 213	ND	ND	ND	ND	ND	ND	213	ND
Harmine	RT 33.0	ND	ND	81.0%	18.59%	91.04%	81.0%	27.5%	11.72%
	m/z 212	ND	ND	212	212	212	212	212	212

ND: not detected. RT: retention time.

the solvent hexane demonstrated the presence of 18 peaks, of which 12 were identified and included hydrocarbons and fatty acids. In the extraction analysis with dichloromethane the presence of 28 peaks was observed, among which it was possible to identify the presence of β-carboline harmine (18.59%), hydrocarbons and stigmasterol fatty acids (6.5%). In the extraction with ethyl acetate solvent, 10 peaks were observed, of which 11% corresponded to fatty acids and 81% corresponding to β-carboline harmine.

In the analysis of the extraction with methanol the presence of 25 peaks was detected, being possible the identification of β-carboline harmine (11.72%), hydrocarbons and their derivatives, stigmasterol fatty acids (2%), as well as triterpene betulin (2%), the latter was also observed in the methanol extraction of whole seed (group A seeds). Table 4 shows the quantitative relationship of the harmaline and harmine compounds present in the fractionated extracts, according to the retention time (RT) and the mass / charge (m/z) ratio of the respective compounds of interest.

Considering the results presented on the analysis performed by solvent partition, it was noticed that the chemical profile of the extraction of the whole or shaved seeds presented the same aspects.

It was possible to identify the β-carbolines harmine and harmaline that have great pharmacological importance. It was observed that after extraction with the solvent methanol was more efficient when compared to the other analyzed solvents (hexane, dichloromethane and ethyl acetate), mainly due to the purity of the peak observed in the chromatogram and the greater amount of the extracted compound. The high polarity of the solvent methanol and its affinity with β-carboline molecules, justifies the most significant separation efficiency when the methanol solvent was used (Martins et al., 2013).

Conclusion

The results obtained on the pharmacognostic evaluation of *P. harmala* showed that the vegetable drug analyzed was of satisfactory quality. The phytochemical evaluation showed the main groups of secondary metabolites present in the species. The chemical characterization of the species performed using GC-MS techniques demonstrated the main compounds present in the *P. harmala* seeds. From the GC-MS it was possible to identify β-carbolines (harmaline and harmine), which have important pharmacological properties, mainly highlighting the iMAO activity and the central nervous system. It was still possible to observe that in the

extraction with the solvent methanol there was a greater efficiency of the compounds separation, and that the harmine compound is found in greater quantity, confirming with information already described. Therefore, this information is important for the standardization of the plant drug, contributing to the use of this data in the future development of a product based on plant material.

CONFLICT OF INTERESTS

The authors have not declared any conflict of interests.

ACKNOWLEDGEMENTS

The authors are grateful to Prof. Dr. N.P. Lopes and I. C. C. Turatti of the University of São Paulo (Ribeirão Preto), Brazil, for support with the GC-MS experiments. We also thank Prof. Dr. J. R. G. S. Almeida from Federal University of São Francisco Valley (UNIVASF), Brazil, as well as CAPES, CNPq, FINEP, FAPESB and FACEPE for financial support.

REFERENCES

Brazil (2010). Pharmacopeia Brazilian, 5. ed. Agência Nacional de Vigilância Sanitária. Brasília: Agência Nacional de Vigilância Sanitária 1:91-199.

Carvalho CC, Turatti ICC, Lopes NP, Salvador MJ, Nascimento AM (2014). Chemical composition and antimicrobial activity of essential oil from Brazilian plants Acanthospermum australe, Calea fruticosa and Mikania glauca. African Journal of Pharmacy and Pharmacology 8(14):392-398.

Couto R, Valgas A, Bara M, Paula J (2009). Physicochemical characterization of leaf dust of *Eugenia dysenterica* Dc. (Myrtaceae).

Cruz H, Gonzalez C, Juárez A, Herrera M, Juarez J (2006). Quantification of the microconstituents formed during solidification by the Newton thermal analysis 60 method. Journal of Materials Processing Technology 178(1-3):128-134.

Firmo W, Menezes V, Passos C, Dias C, Alves L, Dias I (2018). Historical context, popular use and scientific conception on medicinal plants. Caderno de Pesquisa 18 (especial):90-95.

Gobbo–Neto L, Lopes NP (2007). Medicinal plants: factors influencing the content of secondary metabolites. Quimica Nova 30(2):374-381.

Herraiz T, González D, Ancín-Azpilicueta C, Arán VJ, Guillén H (2010). Beta–Carboline alkaloids in Peganum harmala and inhibition of human monoamine oxidase (MAO). Food Chemical Toxicology 48(3):839-845.

Kaskoos RA (2014). Physico–chemical Parameters, Phytochemical Screening and Antioxidant Activity of Seeds of Peganum harmala Collected from Iraq. Asian Journal of Biomedical and Pharmaceutical Sciences 28(4):20-24.

Li S, Chenga X, Wang C (2017). A review on traditional uses, phytochemistry, pharmacology, pharmacokinetics and toxicology of the genus Peganum. Journal of Ethnopharmacology 203:127-162.

Luis GP, Cristina CBT, Virgínia CSM, Flores NF (2015). Quality Control and phytochemical screening of the plant drug of Morus nigra L. leaves (MORACEAE). Journal of Basic and Applied Pharmaceutical Sciences 36(2):90-95.

Martins C, Lopes W, Andrade J (2013). Solubility of organic substances. Quimica Nova 36(8):1248-1255.

Moloudizargari M, Mikaili P, Aghajanshakeri S, Asghari M, Shayegh J (2013). Pharmacological and therapeutic effects of Peganum harmala and its main alkaloids. Pharmacognosy Review 7(14):199-212

Muller SD (2006). Determination of Alkaloids and Flavonoids through HPLC and UV of extracts of Passiflora alata curtis, Passifloraceae–Passionfruit. Itajaí. Dissertation [Pharmaceutical Sciences] – University of the Vale does Itajaí.

Pavia D, Lampman G, Kriz G, Vyvyan J (2010). Introduction to Spectroscopy. 4. ed. São Paulo: Cengage Learning.

Podolak I, Galanty A, Sobolewska D (2010). Saponins as cytotoxic agents: A review. Phytochemistry Reviews 9(3):425-74.

Rodrigues TR (2013). Study of harmonic alkaloids in Passiflora edulis Sims f. flavicarpa Degener (MARACUJÁ AZEDO) by SBSE / CLAE–Dual Flu. São Paulo. Dissertation [Analytical and Inorganic Chemistry] – Institute of Chemistry of São Carlos of the University of São Paulo;.

Santos RG (2007). AYAHUASCA: neurochemistry and pharmacology. Mental Health Alcohol Alcohol Drugs 3(1). http://pepsic.bvsalud.org/scielo.php?script=sci_arttext&pid=S1806-69762007000100007&lng=pt&nrm=iso

Sassoui D, Seridi R, Azin K, Usai M (2005). Evaluation of phytochemical constituents by GC–MS and antidepressant activity of *Peganum harmala* L. seeds extract. Asian Pacific Journal of Tropical Disease 5(12):971-974.

Simões CMO, Schenkel EP, Mello JCP, Mentz LA, Petrovick PR (2017). Pharmacognosy: from the natural product to the drug. Porto Alegre: Artmed,. 486p.

Wagner H, Bladt S (1996). Plant drug analysis: a thin layer chromatography atlas. 2 ed. Berlim Heidelberg: Springer Verlag.

Tavares LS (2014). Investigation of alkaloids B–carbolines, Tryptamine, present in Ayahuasca (Santo Daime) in a sweat sample. Ribeirão Preto. Dissertation.

Tengku MT, Naz H, Jalal R, Hussin K, Abd RM, Adam A (2013). Chemical and pharmacognostical characterization of two Malaysian plants both known as Ajisamat. Brazilian Journal of Pharmacognosy 23:724-730.

Related Journals: